UNIVERSITY OF THESSALY
Department of Civil Engineering

UNIVERSITE JOSEPH FOURIER
Observatoire des Sciences de l'Univers de Grenoble

EVALUATION OF 1-D AND 2-D HYDRAULIC NUMERICAL MODELS FOR FLOOD RISK ASSESSMENT

M.Sc. Management of Hydrometeorological Hazards – HYDROHASARDS

Master thesis submitted by

***D. Plitsi*[1]**

Supervised by

Associate Prof. Evangelia Farsirotou
Dr. LamprosVasiliades

(1) Department of Civil Engineering, University of Thessaly, Pedion Areos, Volos, 38333, Greece
e-mail: dimitraplitsi@gmail.com

January 2016

Institutional Repository - Library & Information Centre - University of Thessaly
20/05/2024 06:18:41 EEST - 3.23.102.234

Acknowledgements

With this master thesis, I would like to thank my supervisors, Associate Prof. Farsirotou Evangelia and Dr. Vasiliades Lampros for their valid help during this study. I would, also, like, to thank Papaioannou George and Dr. Ntassiou Kostantina for the material they offered to me. Most of all, i am very grateful to my family, who has supported me all these months with the best way.

Last but not least, i would like to thank the teaching staff in both universities, University of Thessaly and University Joseph Fourier, for all the valuable knowledge and experience acquired.

Institutional Repository - Library & Information Centre - University of Thessaly
20/05/2024 06:18:41 EEST - 3.23.102.234

ABSTRACT

The aim of this article is to evaluate the results of one-dimensional 1D) and two-dimensional (2D), based on the finite-volume method, hydraulic simulation of a 9 km lowland reach of Titarisios River in Thessaly, Greece. The characteristics of the basin of Titarisios River were estimated with HEC-GeoHms. HEC-HMS software was used to derive the design hydrographs for 50 and 100 years return period by applying three different methods for estimating direct runoff. The geometry of the river was designed in Arcmap GIS environment with the application of HEC-GeoRas, and, then, extracted in HEC-RAS (v. 5.0 Beta), in order to perform unsteady flow analysis for 50 and 100 years flood period, with the 1-D with the domain defined as series of extended cross-sections and 2-D model, with the main channel and the floodplain defined by a series of storage cells. The two-dimensional (2D) model unsteady flow river calculations resulted to a better representation of inundation extent of Titarisios River than the one-dimensional (1D) model.

Keywords: *unsteady flow, one-dimensional hydraulic analysis, two-dimensional hydraulic analysis, inundation mapping, flood risk assessment*

ΠΕΡΙΛΗΨΗ

Σκοπός αυτού του άρθρου είναι να αξιολογηθούν τα αποτελέσματα της μονοδιάστατης και της δισδιάστατης, η οποία βασίζεται στη μέθοδο πεπερασμένου όγκου, υδραυλικής προσομοίωσης 9 χιλιομέτρων (Km) του πεδινού τμήματος του Τιταρήσιου ποταμού της Θεσσαλίας, στην Ελλάδα. Τα χαρακτηριστικά της λεκάνης του Τιταρήσιου ποταμού υπολογίστηκαν με το HEC-GeoHms. Το λογισμικό HEC-HMS χρησιμοποιήθηκε για τον υπολογισμό του πλημμυρικού υδρογραφήματος για περίοδο επαναφοράς 50 και 100 έτη, με την εφαρμογή τριών διαφορετικών μεθόδων για την εκτίμηση της άμεσης απορροής. Η γεωμετρία του ποταμού σχεδιάστηκε στο περιβάλλον ArcMap του GIS, με την εφαρμογή του προγράμματος HEC-GeoRas, και, στη συνέχεια, πραγματοποιήθηκε εξαγωγή της στο HEC-RAS (v. 5.0 Beta), προκειμένου να εκτελέσει προσομοίωση υπό συνθήκες μη μόνιμης ροής, για πλημμυρική περίοδο 50 και 100 έτη, με το μονοδιάστατο μοντέλο να προσομοιώνεται με βάση τις εισαχθείσες διατομές, ενώ η κύρια κοίτη και η πλημμυρική περιοχή στο δισδιάστατο μοντέλο να ορίζεται από ένα πλέγμα κυψελών. Η προσομοίωση της μη μόνιμης ροής με το δισδιάστατο μοντέλο οδήγησε σε καλύτερη αποτύπωση της πλημμυρικής κατάκλυσης του Τιταρήσιου ποταμού σε σύγκριση με το μονοδιάστατο μοντέλο.

Λέξεις-κλειδιά: *μη μόνιμη ροή, μονοδιάστατη υδραυλική προσομοίωση, δισδιάστατη υδραυλική προσομοίωση, χάρτης κατάκλυσης, αξιολόγηση των κινδύνων πλημμύρας*

Institutional Repository - Library & Information Centre - University of Thessaly
20/05/2024 06:18:41 EEST - 3.23.102.234

RESUME

Le but de cet article est d'évaluer les résultats de unidimensionnel (1D) et deux dimensions (2D), qui est basé sur la méthode des volumes finis, simulation hydraulique 9 kilomètres (km) de la partie plate de la rivière Titarisios, en Thessalie, en Grèce. Les caractéristiques du bassin de la rivière Titarisios ont été estimées avec HEC-GeoHms. Le logiciel HEC-HMS a été utilisée pour calculer hydrogramme de crue pour une période de 50 et 100 ans de retour, avec l'application de trois méthodes différentes pour l'estimation de ruissellement direct. La géométrie de la rivière a été conçu dans ArcMap environnement GIS avec l'application de HEC-GeoRas, et, ensuite, extrait de HEC-RAS (v. 5.0 Beta), afin d'effectuer l'analyse des flux instable pour la période de crue 50 et 100 ans de retour, avec le 1-D, avec le domaine défini comme série de sections transversales élargies et le modèle 2-D, avec le canal principal et la plaine inondable défini par une série de cellules de stockage. Les deux dimensions (2D) modèle flux instable calculs de la rivière ont abouti à une meilleure représentation de l'inondation étendue de Titarisios rivière que le (1D) modèle unidimensionnel.

Mots-clés: *écoulement instable, unidimensionnelle analyse hydraulique, analyse hydraulique à deux dimensions, la cartographie des inondations, l'évaluation des risques d'inondation*

Institutional Repository - Library & Information Centre - University of Thessaly
20/05/2024 06:18:41 EEST - 3.23.102.234

CONTENTS

Institutional Repository - Library & Information Centre - University of Thessaly
20/05/2024 06:18:41 EEST - 3.23.102.234

1 INTRODUCTION

Directive 2007/60/EC on the assessment and management of flood risks requires to map the flood extent in all water courses and coast lines which are at risk from flooding and to take adequate and coordinated measures to reduce this flood risk. This Directive also reinforces the rights of the public to access this information and participate in the planning process. The application of a one dimensional (1D) or a two dimensional (2D) hydraulic flood propagation model for flood hazard and risk assessment makes a focus on how well can predict the spatial-dynamic characteristics of floods and how the model results can be transformed into a flood risk assessment.

There are many records of inundations of Titarisios River, which is our case study, situated in Thessaly, Greece. In Mars, 2015, Titarisios River flooding resulted in disrupting traffic in the transport network connecting Ampelonas to Deleria, both situated around 3km south and north, of Titarisios River banks, respectively.

According to Delaney et al (2015), although one of the growth areas in the city of Mississauga, that has recently identified strategic growth, had been included in an update to the regulatory floodplain mapping, the one-dimensional (1D) model that was used to map the floodplain was not capable of representing the complex overland. MIKE FLOOD was selected for a more detailed two dimensional (2D) modeling. Comparison between 1D/1D and 1D/2D Coupled (Sewer/Surface) Hydraulic Models for Urban Flood Simulation (Leandro et al, 2009) shows that flow over the terrain is better modeled by 2D models, whereas in confined channels 1-D models provide a good approximation with less computational effort. Another important development resulting from the modeling needs is the integrated fully implicit approach to the combined 1-D and 2-D modeling of rivers, channels, urban drainage systems and floodplains, such as implemented in the SOBEK simulation modeling software of WL Delft Hydraulics (Verwey, 2001). It is shown by Vojinovica et al (2009), as expected, that in the case of terrains suited to exclusively 1-D models the prediction of flow variables along the channel can be realistic, but that, when it comes to the projection onto a 2D map, the representation of the terrain topography together with the mapping techniques that are employed introduce a limiting factor in their successful application.

The requirement of an accurate inundation mapping has given an impulse to the development of new technologies, such as airborne laser altimetry, used for several years now to monitor efficiently and accurately the floodplain topography (Verwey, 2001). However, recent developments extend the use of laser altimetry technology to the production of flow roughness maps and the monitoring of flood water levels to support model calibration. Comparison of resulting maps for two study areas (Strouds Creek in North Carolina and Brazos River in Texas) shows that the flood inundation area reduces with improved horizontal resolution and vertical accuracy in the topographic data. This reduction is further enhanced by incorporating river bathymetry in topography data (Cook et al, 2009).

In practical application, in our case, one-dimensional (1D) and two-dimensional (2D) unsteady flow analysis by simulating Titarisios River Reach was performed by HEC-RAS, version 5.0 Beta. Two terrains were created by ASTER GDEM v2

Institutional Repository - Library & Information Centre - University of Thessaly
20/05/2024 06:18:41 EEST - 3.23.102.234

Worldwide Elevation Data, in Greek Grid projection , in order to estimate all the factors which were necessary for the simulation.

The first terrain with 20 meters contours interval was used by HEC-GeoHMS program, in Arcmap Gis environment, version 10.1, to compute basin characteristics, such as the area of the subbasins, the slope, concentration time, etc. Moreover, with HEC-GeoHMS the flow network, for the representation of the watershed and the stream was designed. Intensity-Duration-Frequency (IDF) and Depth-Duration-Frequency curves were estimated from the isoyetal map (Sofianopoulos, 1999) for 50 and 100 years return period, and the alternating block model (Chow et al., 1988) was used for the hyetograph, in order to derive synthetic unit hydrographs for the 1-D and 2-D simulations. For the flow hydrographs, SCS, Snyder and Clark methods were followed, simulated with HEC-HMS program. For all methods, time lag had to be computed first. Moreover, SCS method Curve Number and percentage of impervious soil needed to be estimated. Coefficients C_t representing the topographic and soil characteristics of the subbasins and C_p representing the peaking coefficient were essential for the Snyder synthetic unit hydrographs. Storage coefficient was estimated for Clark unit hydrograph. SCS method had the worst design hydrograph, and, thus, was finally selected.

The second terrain created by 1 meter contours interval was required by HEC-GeoRAS, for pre-processing data, such as river reach, banks, or cross-sections and Manning's n value needed for HEC-RAS. Since no topographic data, of the river, were available, this was a mandatory work. One-dimensional (1D) unsteady flow analysis was performed using as upstream boundary conditions SCS synthetic unit hydrograph, for 50 and 100 years flood period, and as downstream boundary conditions normal depth. Initial conditions were set the initial flow of the hydrograph, for 50 years return period, while for 100 years return period, as initial condition a smaller value than the initial flow was set, in order the model to have stability. Similar initial and boundary conditions were set for two-dimensional (2D) unsteady flow analysis, with the difference that a 2D mesh, rather than cross-sections, designed for the simulation. Inundation maps for risk assessment were computed, for 50 and 100 years flood period.

In next chapters, there will be a more detailed description about the setup of the models, and the results, as well as the conclusions will follow.

Institutional Repository - Library & Information Centre - University of Thessaly
20/05/2024 06:18:41 EEST - 3.23.102.234

2 MODEL DESCRIPTION AND SETUP

Titarisios River is located in Thessaly (Fig. 1), Greece, starting from the Olympus mountain at an elevation of 850 meters and ends up in Pinios River (at about 60 meters above sea level). The length of the river is 70 Km, in approximation, and its basin is 1800km2.

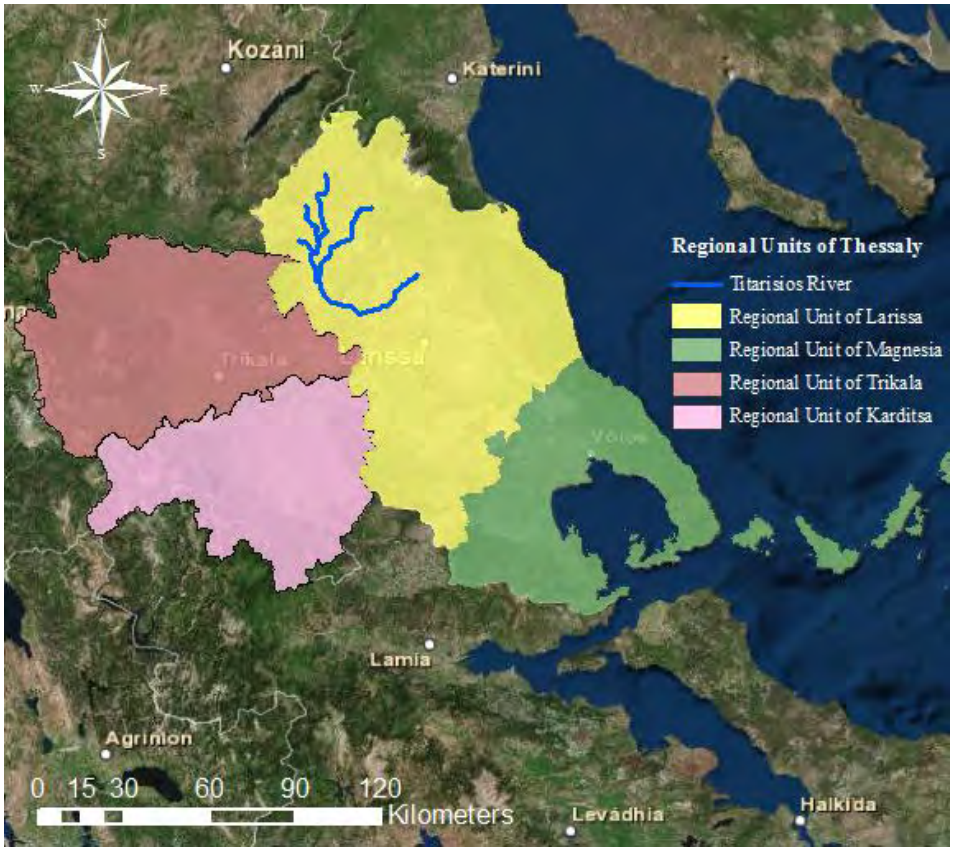

Figure 1. Regional Units of Thessaly, where Titarisios River is situated.

In Fig. 2, Titarisios River has been emerged from a DEM, with a 20m contours interval.

Institutional Repository - Library & Information Centre - University of Thessaly
20/05/2024 06:18:41 EEST - 3.23.102.234

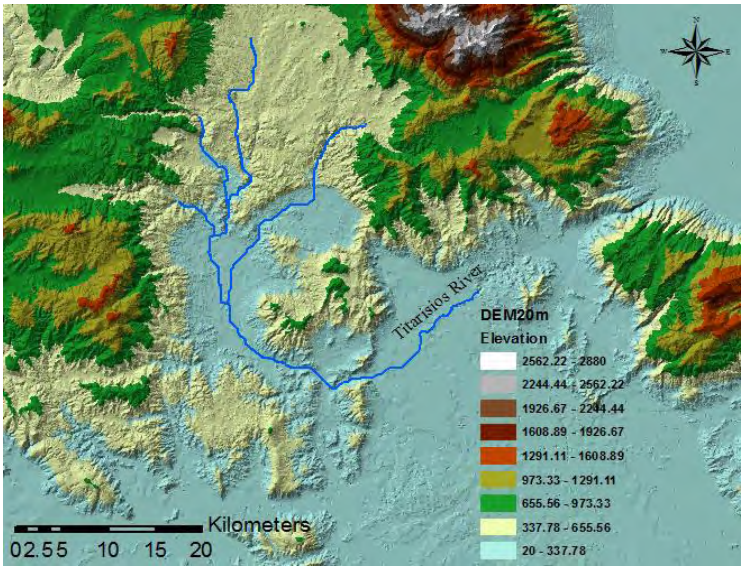

Figure 2. Representation of Titarisios River with a DEM of 20m interval contours.

As we mentioned above, an accurate digital elevation model (DEM) is appropriate in order to succeed a good approach of the inundation extent. Global Mapper simulated contours with 20 meters interval from ASTER GDEM v2 Worldwide Elevation Data, in Greek Grid projection. HEC-GeoHMS is based on the DEM to simulate the basin of Titarisios River, and basin characteristics, such as subbasins, elevation of the subbasins, stream length, area and slope of the subbasins, longest flowpaths, centroids and cendroidal longest flowpaths of the three subbasins.

2.1 Estimation of basin characteristics

All basin characteristics have been estimated in Arcmap Gis environment (Figure 3. and Figure 4) with HEC-GeoHMS (Table 1).

Institutional Repository - Library & Information Centre - University of Thessaly
20/05/2024 06:18:41 EEST - 3.23.102.234

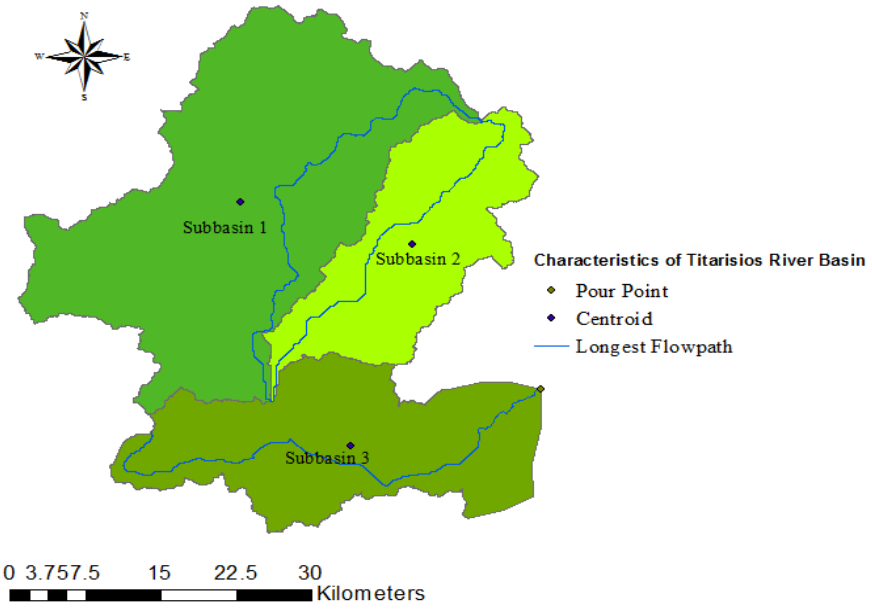

Figure 3. Longest flowpath of each subbasin of Titarisios River, Thessaly.

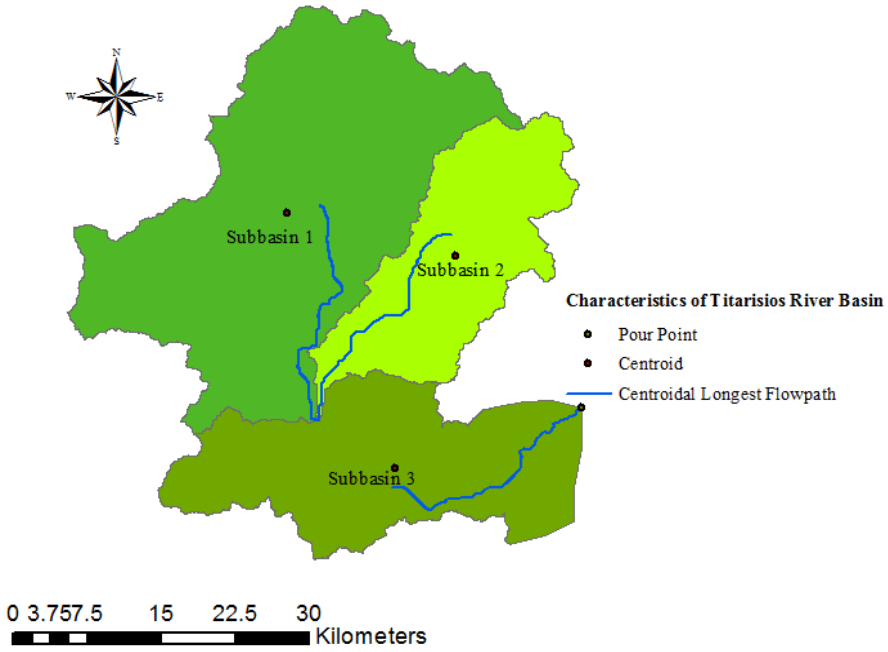

Figure 4. Centroidal longest flowpath of each subbasin of Titarisios River, Thessaly.

Institutional Repository - Library & Information Centre - University of Thessaly
20/05/2024 06:18:41 EEST - 3.23.102.234

Table 1. Basin characteristics of Titarisios River

	Subbasin 1	Subbasin 2	Subbasin 3
Area, A, (km2)	928.33	376.36	526.05
Perimeter, P_e, (km)	248.82	157.62	180.71
Maximum Elevation, H_{max}, (m)	2580.00	2580.00	1220.00
Mean Elevation, H_{mean}, (m)	488.62	667.16	299.58
Minimum Elevation, H_{min}, (m)	140.00	140.00	60.00
Longest watercourse from the point of concentration to the boundary of the drainage basin, L, (km)	60.23	47.83	57.13
Length along the longest watercourse from the point of concentration to a point opposite the centroid of the drainage basin, L_c (km)	28.43	28.02	24.31
(Maximum Elevation (m)-Minimum Elevation (m))/ Length along the longest watercourse from the point of concentration to a point opposite the centroid of the drainage basin L_C (km), S	0.20	0.22	0.15

2.1.1 Giandotti formula

Concentration time is the time for the runoff to become established and flow from the most remote part of the drainage area to drainage outlet. The Giandotti formula gives higher values for the time of concentration compared to the Kirpich formula, and presented as:

$$t_c = \frac{4\sqrt{A} + 1.5L}{0.8\sqrt{\Delta H}} \quad (1)$$

where t_c is the concentration time (hrs), A is the drainage area (Km^2), L the length of the main watercourse (Km) and ΔH the elevation difference of the average basin elevation from the outlet elevation (m). Using Giantotti formula for the basin of Titarisios River, concentration time was estimated (Table 2).

Institutional Repository - Library & Information Centre - University of Thessaly
20/05/2024 06:18:41 EEST - 3.23.102.234

Table 2. Basin characteristics of Titarisios River

	Subbasin 1	Subbasin 2	Subbasin 3
Concentration time (hrs)	14.21	8.13	14.33

2.2 Intensity-duration-frequency relationship

An attempt to adjust and apply a methodology to the development of the maximum rainfall-duration-frequency (IDF) curves in large geographical areas has been made. The methodology takes advantage not only of the data from recording rain-gauges, but also, of the dense network of non-recording rain-gauges in Thessaly (Sofianopoulos, 1999). Thessaly has been divided in three zones and fixed values have been given in 2 out of 4 parameters of each zone. By using the isoyetal maps, it is possible to extend relationship to every single place of the area. Titarisios River belongs to zone III (Fig. 5), and uses the IDF relationship of Tyrnavos (Equation 8), for 50 and 100 year return period.

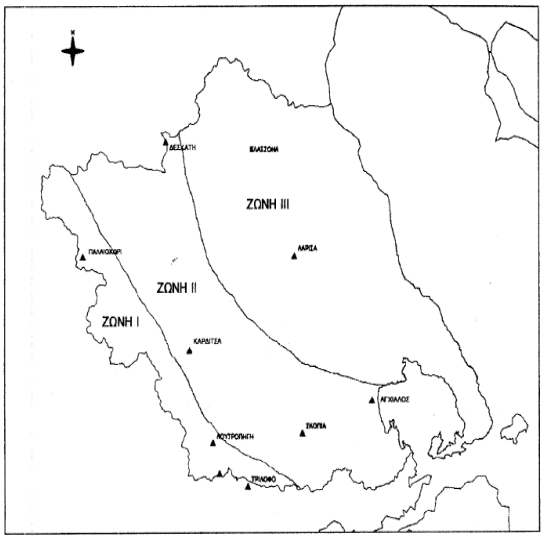

Figure 5. Separation of Thessaly in zones I, II and III (Sofianopoulos, 1999).

In order to estimate the rainfall amount in the basin of Titarisios River, we use the intensity-duration-frequency (IDF) relationship from Gumbel distribution function. The parameters of the function were estimated with L-Moments method (Equations 6 and 7).

2.2.1 Cumulative distribution function

To describe the probability distribution of a random variable, the CDF (Cumulative Distribution Function) is used. The value of this function $F_X(x)$ is the probability P of the event that the random variable takes on values equal to or less than a specific value x. Therefore the function is considered as a non exceedance probability. The function

Institutional Repository - Library & Information Centre - University of Thessaly
20/05/2024 06:18:41 EEST - 3.23.102.234

$F_X(x)$ is the probability that during the year the random variable X will not exceed some x, given as:

$$F_X(x) = P[X \le x] \tag{2}$$

2.2.2 Probability density function

The probability density function (PDF) of X is related to F(x) as:

$$F(x) = \int_{-\infty}^{x} f(t)dt \tag{3}$$

Statistical distribution Gumbel was applied. The parameters of the distribution were estimated, and the Cumulative Density Function (CDF) and Probability Density Function (PDF) were created, according to Hosking equations (1977).

The corresponding probability density functions, generated as derivatives of the probability distribution functions are:

$$f_{\xi,\mu,\sigma}(x) = \frac{1}{\sigma}\left(1+\xi\frac{(x-\mu)}{\sigma}\right)^{-1-1/\xi} \exp\left(-\left(1+\xi\frac{(x-\mu)}{\sigma}\right)^{-1/\xi}\right) \tag{4}$$

for $\xi \neq 0$, and

$$f_{\xi,\mu,\sigma}(x) = \frac{1}{\sigma}e^{-(x-\mu)/\sigma} \exp\left(-e^{-(x-\mu)/\sigma}\right) \tag{5}$$

for $\xi = 0$

2.2.3 Method of L-moments

L-moments are based on probability-weighed moments (PWMs), and have simple interpretations of location, dispersion, skewness, kurtosis, and other aspects of the shape of probability distributions or data samples. It almost always produces some asymptotically unbiased estimators. Thus, if:

$$b_o = \frac{1}{n}\sum_{j=1}^{n} X_{j:n} \tag{6}$$

$$b_o = \frac{1}{n}\sum_{j=r+1}^{n} \frac{(j-1)(j-2)\ldots(j-r)}{(n-1)(n-2)\ldots(n-r)} x_{j:n} \tag{7}$$

Institutional Repository - Library & Information Centre - University of Thessaly
20/05/2024 06:18:41 EEST - 3.23.102.234

2.2.4 IDF curve

Intensity-duration–frequency (IDF) relationship of rainfall amounts is one of the most commonly used tools in water resources engineering for planning, design and operation of water resources projects. The equation used is described as below:

$$i = \frac{\frac{1}{\lambda}\left\{\psi - \ln\left[-\ln\left(1-\frac{1}{T}\right)\right]\right\}}{(d+f)^n} \tag{8}$$

where i is the intensity of the rain (mm/h), d is the duration of the rain (hrs), T is the return period (years), f, n, ψ, and λ are the coefficients, different for each station

For zone III, fixed coefficients f and n are equal to f=0.2 and n=0.78. From the isoyetal map (Sofianopoulos, 1999) coefficients ψ and λ are equal to ψ=3.545, and λ=0.152. For all subbasins of Titarisios River (Subbasin 1, 2 and 3) and for 50 and 100 years flood period, in Table 3, intensity of the rain in mm is given.

Table 3. Rainfall intensity for 50 and 100 yrs flood period, for the basins of Titarisios River

	Subbasin 1	Subbasin 2	Subbasin 3
i_{50} (mm/h)	6.13	9.40	6.09
i_{100} (mm/h)	6.71	10.29	6.67

2.2.5 Rainfall amount

For the estimation of the rainfall amount for 50 and 100 years flood period the following equation is used:

$$h(T) = i * d \tag{9}$$

where i is the intensity of the rain (mm/h), d is the duration of the rain (hrs), $h(T)$ is the rainfall amount depended on the return period (mm)

As mentioned above, by using the data of recording rain-gauges (9 stations, Sofianopoulos, 1999) and non-recording rain-gauges (30 stations, Sofianopoulos, 1999), maximum rainfall depths for various rainfall duration and return period can be estimated (Table 4).

Table 4. Rainfall depth for 50 and 100 yrs flood period, for the basins of Titarisios River

	Subbasin 1	Subbasin 2	Subbasin 3
h_{50}(T) (mm)	87.15	76.46	87.32
h_{100}(T) (mm)	95.32	83.63	95.51

Institutional Repository - Library & Information Centre - University of Thessaly
20/05/2024 06:18:41 EEST - 3.23.102.234

2.3 Synthetic unit hydrographs

A synthetic unit hydrograph retains all the features of the unit hydrograph, but does not require rainfall-runoff data. A synthetic unit hydrograph is derived from theory and experience, and its purpose is to simulate basin diffusion by estimating the basin lag based on a certain formula or procedure. A synthetic unit hydrograph is estimated because there are no runoff data in Titarisios River (no discharge or stage gages). The alternating block model (Chow et al., 1988) was used for the design storm hyetograph (Table A1, A2, Appendix), in order to use it for the synthetic unit hydrograph. Rainfall depth is distributed every 15 min, and total duration of rainfall is t_c = 14.5 hrs, and is bigger than the concentration time estimated in Subbasin 3, for 50 and years flood period. Concentration time, estimated in Subbasin 3, was selected because is the highest of all the subbasins. Correction coefficient φ was used to correct the estimated rainfall as:

$$\phi = 1 - \frac{0.048 * \mathrm{A}^{0.36-0.01*\ln A}}{d^{0.35}} \tag{10}$$

where φ is the correction coefficient of the distributed, every 15 min, rainfall, A is the area of the basin, d is the 15min duration of the distributed rainfall

The dimensionless unit hydrographs of: 1) SCS (Soil Conservation Service), 2) Snyder, and 3) Clark, and together with the distributed total rainfall amount for a flood return period of 50 and 100 years will be used to construct the synthetic unit hydrographs corresponding to the selected rainfall duration.

2.3.1 SCS synthetic unit hydrograph

The dimensionless unit hydrograph used by the SCS was developed by Victor Mockus (1972) and was derived based on a large number of unit hydrographs from basins that varied in characteristics such as size and geographic location. The unit hydrographs were averaged and the final product was made dimensionless by considering the ratios of q/q_p (flow/peak flow) on the ordinate axis and t/t_p (time/time to peak) on the abscissa, where the units of q and q_p are flow/meters of runoff/unit area. This method uses the non-dimensional hydrograph constructed for the SCS area. The formulas of SCS unit are describing below:

$$t_L = \frac{2.587 * L^{0.8}\left(\frac{1000}{CN} - 9\right)^{0.7}}{1900 * H^{0.5}} \tag{11}$$

where t_L is the lag time (hrs), L is the longest watercourse from the point of concentration to the boundary of the drainage basin (km), H is the mean elevation of the drainage basin (m) and CN (Table A3, Appendix) is a the runoff curve number (35<CN<99)

Because each basin has more than one Corine Land Cover class and more than one hydrologic soil type, mean CN_{II} is estimated in order to obtain the curve number for each basin as:

Institutional Repository - Library & Information Centre - University of Thessaly
20/05/2024 06:18:41 EEST - 3.23.102.234

$$CN_{II\,mean} = \frac{\sum A_i * CN_{II\,i}}{\sum A_i} \quad (12)$$

The results of CN_{IImean} and, also, the percentage of the impervious areas (where CN is more than 98) are presented in Table 5.

Hydrolithology map of the area is, also, used, in order to estimate hydrologic soil type. The area is primarily developed for agriculture use. The soil is consisted of flysch impermeable and granular terittories. The area seems to exhibit a relatively medium runoff potential, as Table 5 shows.

Table 5. CN_{IImean} and (%) impervious for the subbasins of Titarisios River, Thessaly

	SCS method		
	Subbasin 1	Subbasin 2	Subbasin 3
CN_{II}	72.02	71.71	67.13
(%) impervious	0.000	0.000	0.069

$$t_0 = \frac{t_L}{5.5} \quad (13)$$

where t_0 is the duration of the excess rainfall (hrs), t_L is the lag time (hrs).

$$t_p = t_L + \frac{t_0}{2} \quad (14)$$

where t_p is the peak time of synthetic hydrograph, t_L is the lag time (hrs), t_0 is the duration of the excess rainfall (hrs).

$$Q = 0.75\left[\frac{A \times P_e}{3600 t_p}\right] \quad (15)$$

where Q is the peak flow discharge (m^3/sec), A is the area (stremma), t_p is the peak time of synthetic hydrograph (hrs)

2.3.2 Snyder synthetic unit hydrograph

The dimensionless unit hydrograph used by the Snyder was derived based on a large number of unit hydrographs from basins that varied in characteristics such as size and geographic location. The unit hydrographs were averaged and the final product was made dimensionless by considering the ratios of q/q_p (flow/peak flow) on the ordinate axis and t/t_p (time/time to peak) on the abscissa, where the units of q and q_p are flow/meters of runoff/unit area. This method uses the non-dimensional hydrograph constructed for the Snyder area. The formulas of SCS unit are describing below:

$$t_L = 0.756 C_t \left(L \times L_{ca}\right)^{0.3} \quad (16)$$

Institutional Repository - Library & Information Centre - University of Thessaly
20/05/2024 06:18:41 EEST - 3.23.102.234

where t_L is the lag time (hrs), L is the longest watercourse from the point of concentration to the boundary of the drainage basin (km), L_{ca} is the length along the longest watercourse from the point of concentration to a point opposite the centroid of the drainage basin (km) and C_t is a coefficient ($1.8<C_t<2.2$)

$$t_0 = \frac{t_L}{5.5} \tag{17}$$

where t_0 is the duration of the excess rainfall (h), t_L is the lag time (hrs)

$$t_p = t_L + \frac{t_0}{2} \tag{18}$$

where t_p is the peak time of synthetic hydrograph, t_L is the lag time (hrs) , t_0 is the duration of the excess rainfall (hrs)

$$Q = 0.75\left[\frac{A \times P_e}{3600 t_p}\right] \tag{19}$$

where Q is the peak flow discharge (m^3/sec), A is the area (stremma), t_p is the peak time of synthetic hydrograph (hrs)

C_t coefficient represents the topographic and soil characteristics of the subbasins and C_p represents the peaking coefficient, and is inversely proportional to C_t (Table 6).

Table 6. C_t and C_p coefficients for the three subbasins of Titarisios River

	Snyder method		
	Subbasin 1	Subbasin 2	Subbasin 3
C_t	2.00	1.90	2.10
C_p	0.62	0.67	0.57

2.3.3 Clark synthetic unit hydrograph

The formulas of Clark unit hydrograph are describing below:

$$t_L = t_c \tag{20}$$

where t_L is the lag time (hrs), t_c is the concentration time (hrs) from Giandotti formula (Equation 1).

$$R = 1.165 t_c \tag{21}$$

where R is the storage coefficient [Technical Documentation for use of Hec-HMS with the Development Process Manual, (Table 7)], t_c is the concentration time (hrs) from Giandotti formula (Equation1)

Institutional Repository - Library & Information Centre - University of Thessaly
20/05/2024 06:18:41 EEST - 3.23.102.234

Table 7. Storage coefficient R for the subbasins of Titarisios River, Thessaly

	Clark method		
	Subbasin 1	Subbasin 2	Subbasin 3
R (hrs)	16.55	9.47	16.69

The time lag that is used for the synthetic unit hydrographs of the three methods, Snyder, Clark and SCS, is shown in Table 8, respectively.

Table 8. Time lag for SCS, Snyder, and Clark method for the subbasins of Titarisios River, Thessaly

	t_L (hrs)		
	Subbasin 1	Subbasin 2	Subbasin 3
SCS method	6.10	4.90	7.71
Snyder method	14.11	12.46	13.92
Clark method	14.21	8.13	14.33

2.3.4 Watershed runoff process for synthetic unit hydrographs

HEC-HMS hydraulic simulation program will be used in order to derive the synthetic unit hydrographs. Figure 6 is a system diagram of the watershed runoff process, at a scale that is consistent with the scale modelled well with the program. The processes illustrated begin with precipitation.

Institutional Repository - Library & Information Centre - University of Thessaly
20/05/2024 06:18:41 EEST - 3.23.102.234

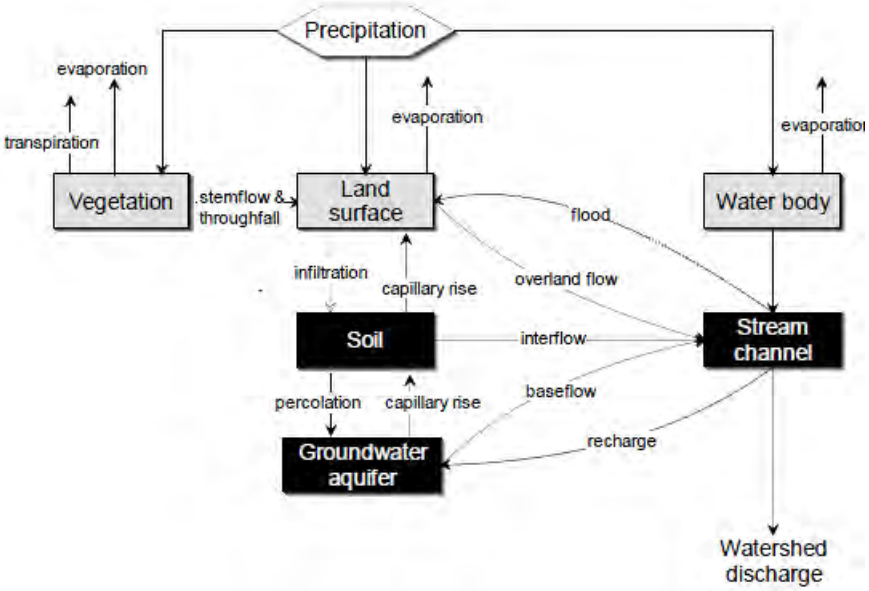

Figure 6. Systems diagram of the runoff process at local scale (after Ward, 1975).

As illustrated in Figure 7, only those components necessary to predict are presented in detail, and the other components are omitted or lumped.

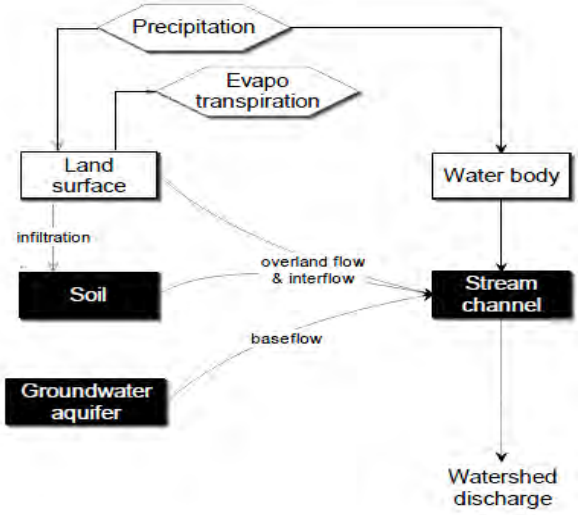

Figure 7. Typical representation of watershed runoff.

The flow network is the skeleton that connects hydrologic elements together into a representation of the stream in the watershed. Each link in the network is a one-way

Institutional Repository - Library & Information Centre - University of Thessaly
20/05/2024 06:18:41 EEST - 3.23.102.234

connector that takes outflow from an element and connects it as inflow to a downstream element. The connection information of the flow network along with the drainage area at each element is used to sort the elements in hydrologic order. In Figure 8, Subbasins 1 (W410) and 2 (W370) are connected with the basin connectors to the Subbasin 3 (W440), downstream the junction (J233). Titarisios River Reach (R120) is a downstream element with two inflows and one outflow. The outlet of the watershed is named Out Titarisios.

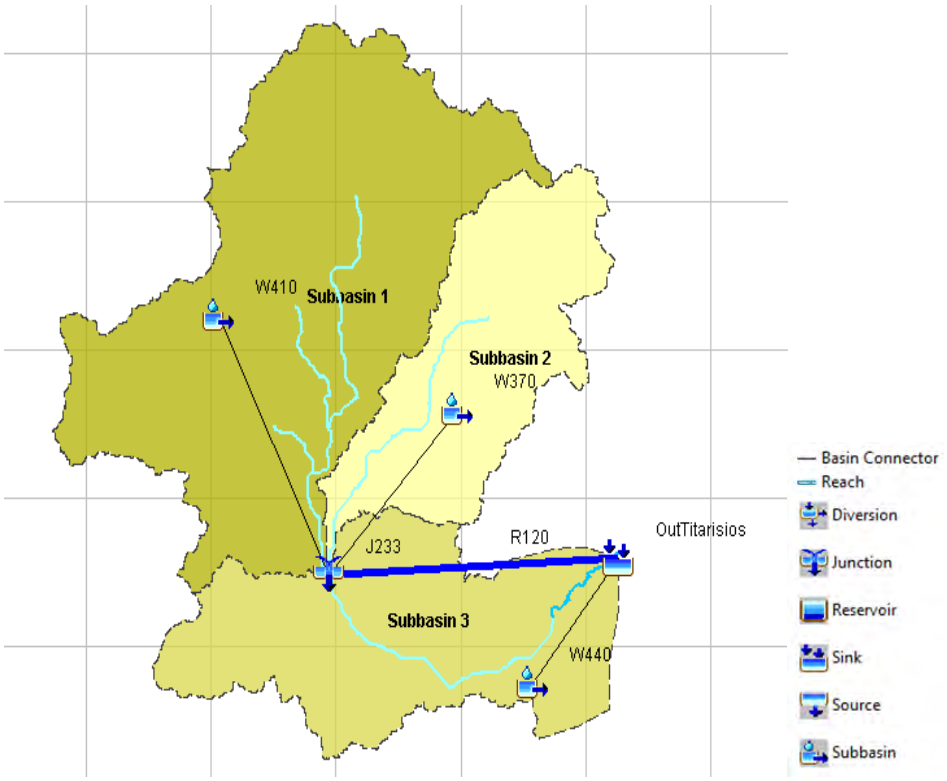

Figure 8. Model of drainage area of Titarisios River, Thessaly.

The unit hydrograph (UH) is well-known, commonly – used empirical of the relationship of direct runoff to excess precipitation. As originally proposed by Sherman in 1932, it is the basin outflow resulting from one unit of direct runoff generated uniformly over the drainage area at a uniform rainfall rate during specified period of rainfall duration. The underlying concept of the UH is that the runoff process is linear, so that the runoff from greater or less than one unit is simply multiple of the unit runoff hydrograph. The results of the simulation with HEC-HMS of the direct runoff hydrographs with a UH (SCS unit hydrograph) can be represented in Figures 9, 10, and 11, for 50 years flood period, and 12, 13, and 14, for 100 years flood period, for Subbasins 1 (W410), 2 (W370), and 3 (440), respectively. Note that SCS UH model assumes that the watershed UH is a single-peaked hydrograph.

Institutional Repository - Library & Information Centre - University of Thessaly
20/05/2024 06:18:41 EEST - 3.23.102.234

Moreover, the SCS Curve Number Loss method implements the curve number methodology for incremental losses. The method calculates incremental precipitation during a storm by recalculating the infiltration volume at the end of each time interval. Infiltration during each time interval is the difference in volume at the end of two adjacent time intervals. Respectively with the SCS transform method, equation 12 results to the Table 5, representing the CN_{IImean} and percentage of the impervious soil of each subbasin of Titarisios River.

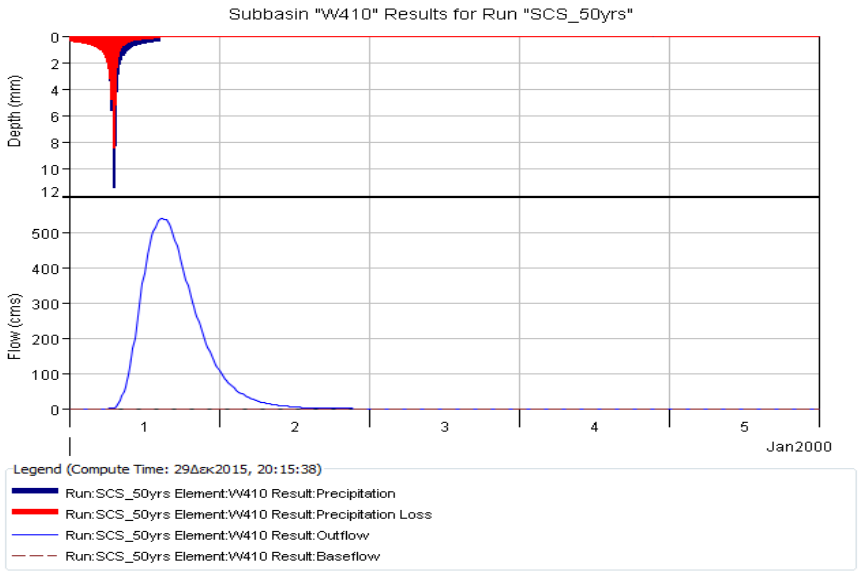

Figures 9. Direct runoff hydrograph of Subbasin 1 (W410), for 50 years flood period of Titarisios River, Thessaly, with SCS synthetic unit hydrograph.

Institutional Repository - Library & Information Centre - University of Thessaly
20/05/2024 06:18:41 EEST - 3.23.102.234

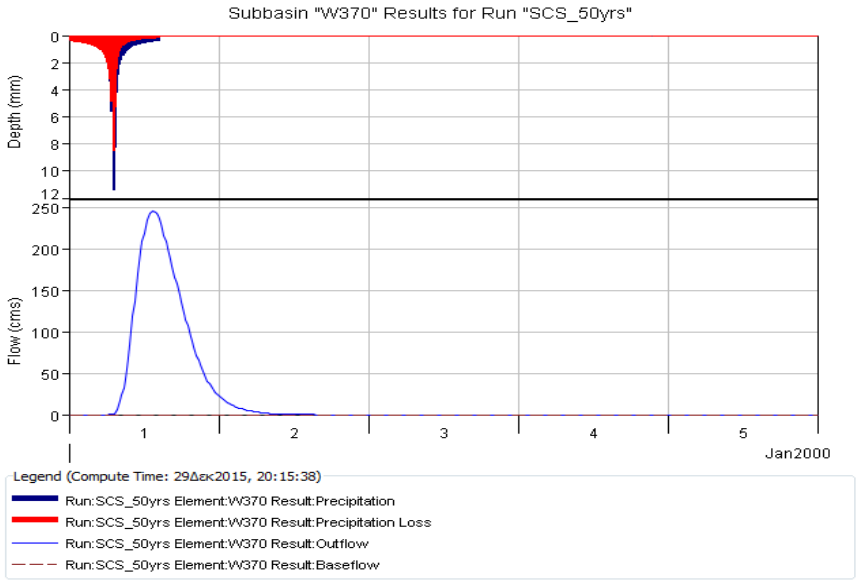

Figure 10. Direct runoff hydrograph of Subbasin 2 (W370), for 50 years flood period of Titarisios River, Thessaly, with SCS synthetic unit hydrograph.

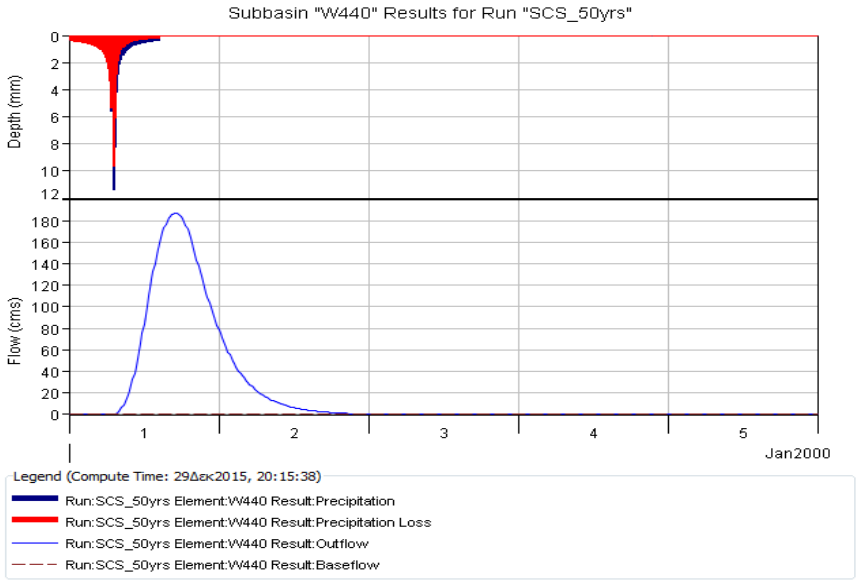

Figures 11. Direct runoff hydrograph of Subbasin 3 (W440), for 50 years flood period of Titarisios River, Thessaly, with SCS synthetic unit hydrograph.

Institutional Repository - Library & Information Centre - University of Thessaly
20/05/2024 06:18:41 EEST - 3.23.102.234

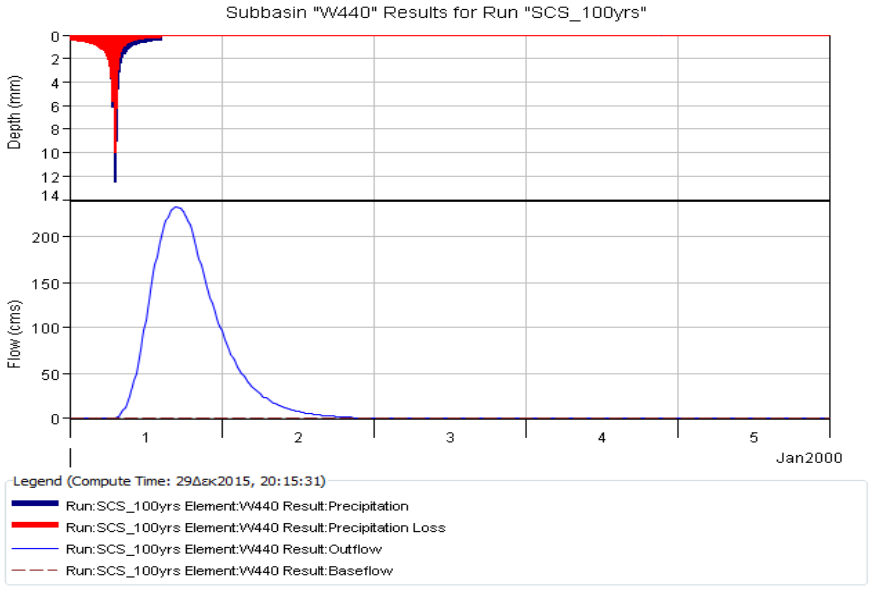

Figure 12. Direct runoff hydrograph of Subbasin 1 (W410), for 100 years flood period of Titarisios River, Thessaly, with SCS synthetic unit hydrograph.

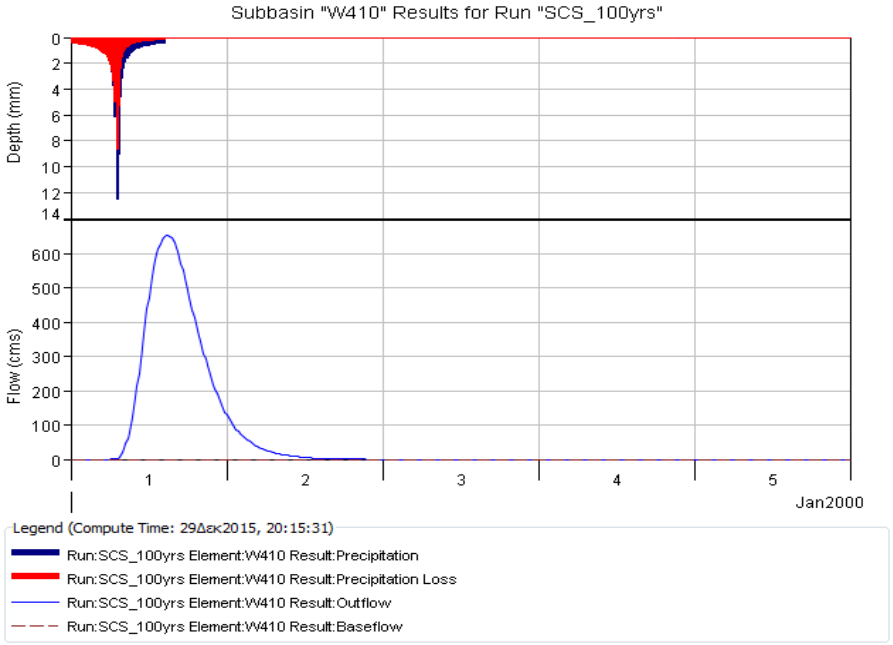

Figure 13. Direct runoff hydrograph of Subbasin 2 (W370), for 100 years flood period of Titarisios River, Thessaly, with SCS synthetic unit hydrograph.

Institutional Repository - Library & Information Centre - University of Thessaly
20/05/2024 06:18:41 EEST - 3.23.102.234

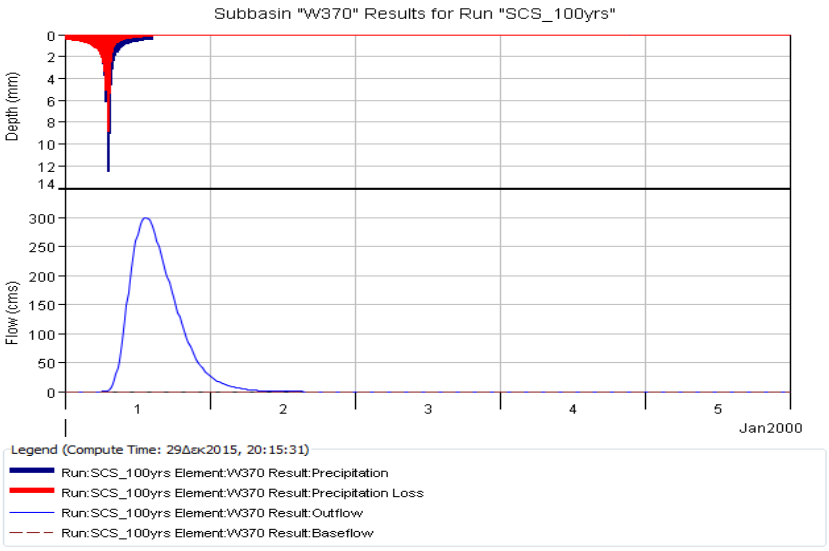

Figure 14. Direct runoff hydrograph of Subbasin 3 (W440), for 100 years flood period of Titarisios River, Thessaly, with SCS synthetic unit hydrograph.

A reach is an element with one or more inflow and only one outflow. If there is more than one inflow, all inflow is added together, before computing the outflow. In our case study, at a stream junction (J233, Figure 8), two channels intersect, flow is combined, and water travels downstream. HEC-HMS follows a simplification of the continuity equation. The downstream flow at the time t equals to the sum of upstream flows. This equation is solved repeatedly for all times t in the simulation duration. The hydrographs from Subbasins 1 (W410) and 2 (W370) which are connected with the basin connectors to the Subbasin 3 (W440) with a junction (J233), give the total outflow with SCS method as shown in Figures 15 and 16, for 50 and 100 years flood period, respectively.

Institutional Repository - Library & Information Centre - University of Thessaly
20/05/2024 06:18:41 EEST - 3.23.102.234

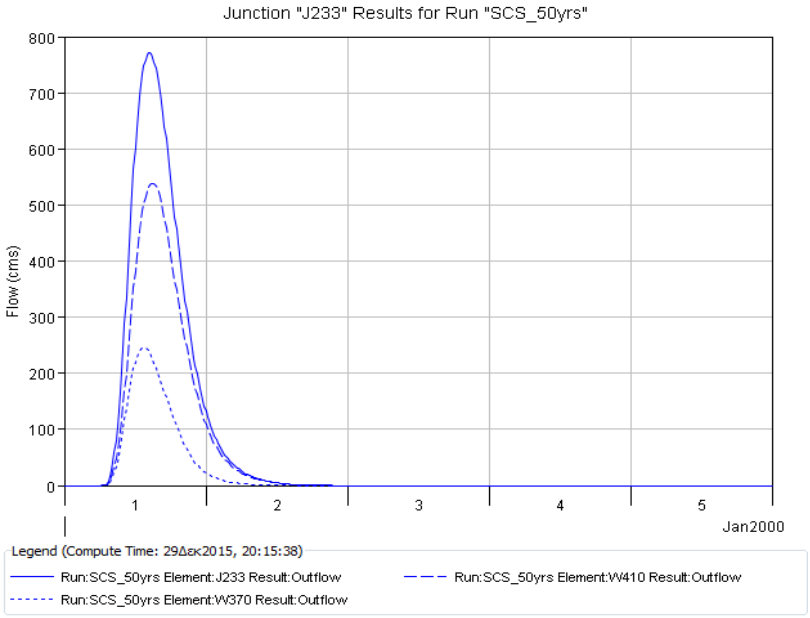

Figure 15. Total hydrograph at the junction (J233) of Subbasins 1 (W410) and 2 (W370) with SCS method, for 50 years flood period of Titarisios River, Thessaly.

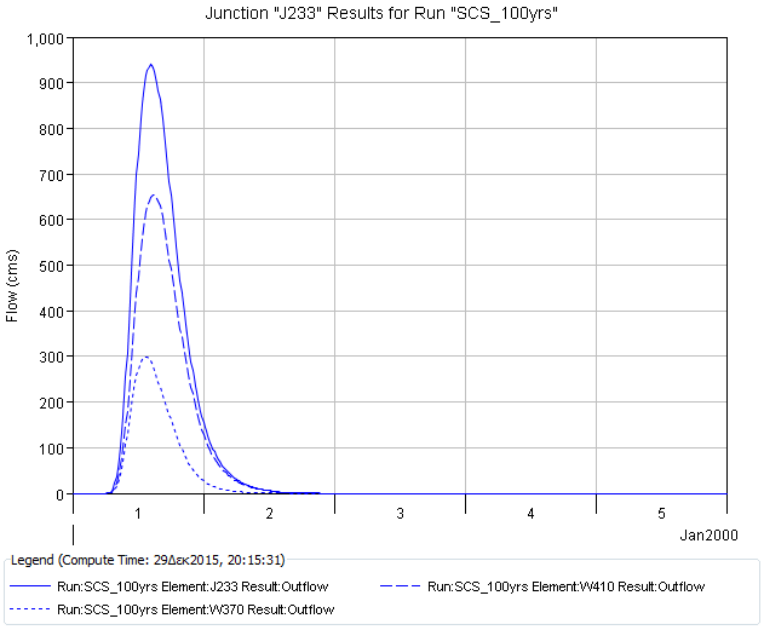

Figure 16. Total hydrograph at the junction (J233) of Subbasins 1 (W410) and 2 (W370) with SCS method, for 100 years flood period of Titarisios River, Thessaly.

Institutional Repository - Library & Information Centre - University of Thessaly
20/05/2024 06:18:41 EEST - 3.23.102.234

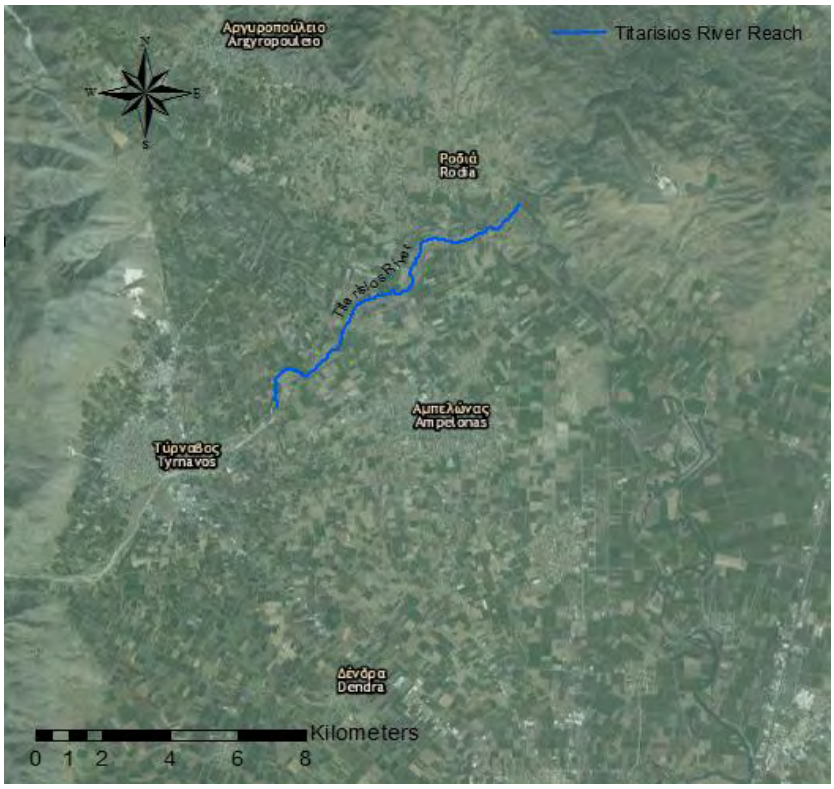

Figure 17. Representation of Titarisios River Reach, Thessaly.

The reach element is used to model Titarisios River Reach (Figure 17). In model drainage (Figure 8) the reach (R120) will be used for the simulation of the open channel. The Muskingum-Cunge routing method is based on the combination of the conservation of mass approach and the diffusion representation of the conservation of momentum, to route flow through the reach stream. It is sometimes referred to as variable coefficient method, because the routing parameters are recalculated every time step, based on channel properties and flow depth. It represents attenuation of flood waves and can be used in reaches with small slope, as in our case. The length of Titarisios River in our study is 8943.20 meters, and the slope of the reach is 0.005. Manning coefficient for the channel is equal to 0.04, for water courses, beaches dunes, and sands, the shape of the river is trapezoid, with side slope equal to 0.04 (xH:1V), and bottom width 100 meters in approximation. None loss-gain method was selected, including any losses or gains to the channel.

The model is based upon solution of the following form of the continuity equation, with lateral q_l inflow included:

$$\frac{\partial A}{\partial t} + \frac{\partial Q}{\partial x} = q_L \tag{22}$$

Institutional Repository - Library & Information Centre - University of Thessaly
20/05/2024 06:18:41 EEST - 3.23.102.234

and the diffusion form of the momentum equation:

$$S_f = S_o - \frac{\partial y}{\partial x} \tag{23}$$

Combining these and using a linear approximation yields the convective diffusion equation (Miller and Cunge, 1975):

$$\frac{\partial Q}{\partial t} + c\frac{\partial Q}{\partial x} = \mu\frac{\partial^2 Q}{\partial x^2} + cq_L \tag{24}$$

where c is wave celerity (speed), and μ is hydraulic diffusivity

The wave celerity and the hydraulic diffusivity are expressed as follows:

$$c = \frac{dQ}{dA} \tag{25}$$

and

$$\mu = \frac{Q}{2BS_O} \tag{26}$$

where B is the top width of the water surface

A finite difference approximation of the partial derivatives, combined with the following equation:

$$Q_t = \left(\frac{\Delta t - 2KX}{2K(1-X)+\Delta t}\right)I_t + \left(\frac{\Delta t + 2KX}{2K(1-X)+\Delta t}\right)I_{t-1} + \left(\frac{2K(1-X)-\Delta t}{2K(1-X)+\Delta t}\right)Q_{t-1} \tag{27}$$

will be:

$$Q_t = C_1 I_{t-1} + C_2 I_t + C_3 Q_{t-1} + C_4(q_L \Delta x) \tag{28}$$

The coefficients are:

$$C_1 = \frac{\frac{\Delta t}{K} + 2X}{\frac{\Delta t}{K} + 2(1-X)} \tag{29}$$

$$C_2 = \frac{\frac{\Delta t}{K} - 2X}{\frac{\Delta t}{K} + 2(1-X)} \tag{30}$$

Institutional Repository - Library & Information Centre - University of Thessaly
20/05/2024 06:18:41 EEST - 3.23.102.234

$$C_3 = \frac{2(1-X) - \frac{\Delta t}{K}}{\frac{\Delta t}{K} + 2(1-X)} \tag{31}$$

$$C_4 = \frac{2\left(\frac{\Delta t}{K}\right)}{\frac{\Delta t}{K} + 2(1-X)} \tag{32}$$

The parameters K and X are (Cunge, 1969; Ponce, 1978):

$$K = \frac{\Delta x}{c} \tag{33}$$

$$X = \frac{1}{2}\left(1 - \frac{Q}{BS_o c \Delta x}\right) \tag{34}$$

But c, Q and B change over time, so the coefficients C_1, C_2, C_3, and C_4 must, also change, and recomputed at each time and distance step, Δt and Δx, using the algorithm proposed by Ponce (1989). Δx is computed as:

$$\Delta x = c\Delta t \tag{35}$$

The value is constrained so that:

$$\Delta x < \frac{1}{2}\left(c\Delta t + \frac{Q_o}{BS_o c}\right) \tag{36}$$

where Q_o is reference flow, computed from the inflow hydrograph as:

$$Q_o = Q_B + \frac{1}{2}\left(Q_{peak} - Q_B\right) \tag{37}$$

where Q_B is the baseflow and Q_{peak} is the inflow peak

The following Figures (Figures 18, 19, 20, 21, 22, and 23 represent ***final*** design hydrographs with SCS, Snyder and Clark methods used in Muskingum-Cunge routing method, with no loss method, for 50 and 100 years flood period, respectively, of Titarisios River Reach.

Institutional Repository - Library & Information Centre - University of Thessaly
20/05/2024 06:18:41 EEST - 3.23.102.234

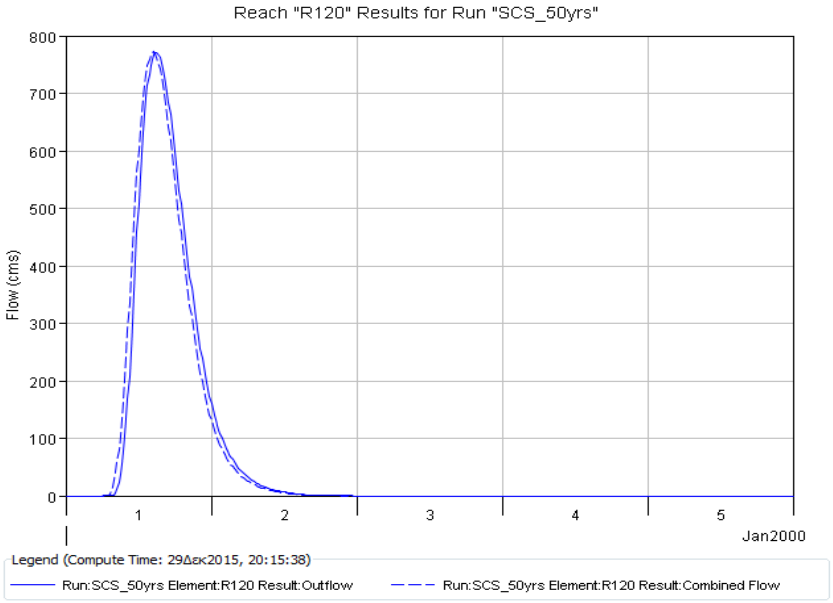

Figure 18. Final design hydrograph with SCS method used for Muscingum – Cunge route method for 50 years flood period of Titarisios River, Thessaly.

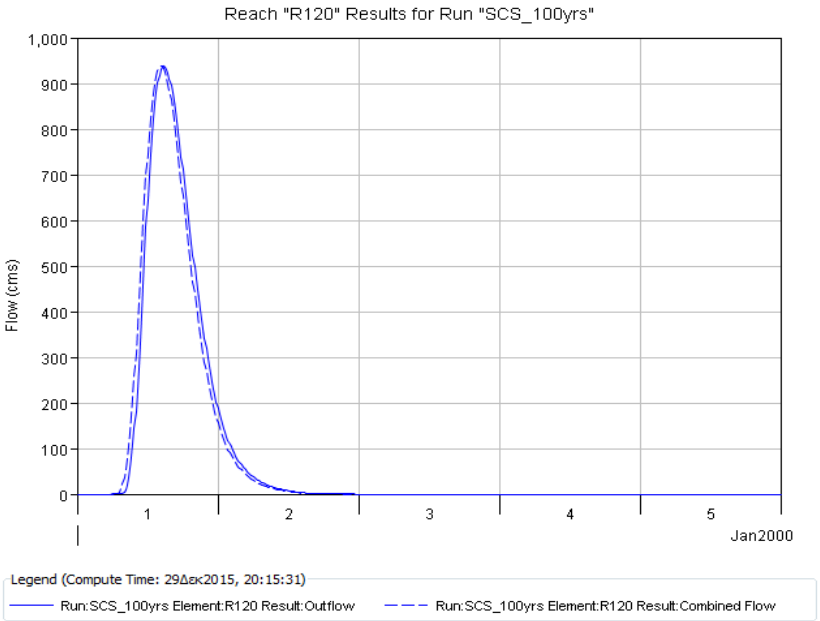

Figure 19. Final design hydrograph with SCS method used for Muscingum – Cunge route method for 100 years flood period of Titarisios River, Thessaly.

Institutional Repository - Library & Information Centre - University of Thessaly
20/05/2024 06:18:41 EEST - 3.23.102.234

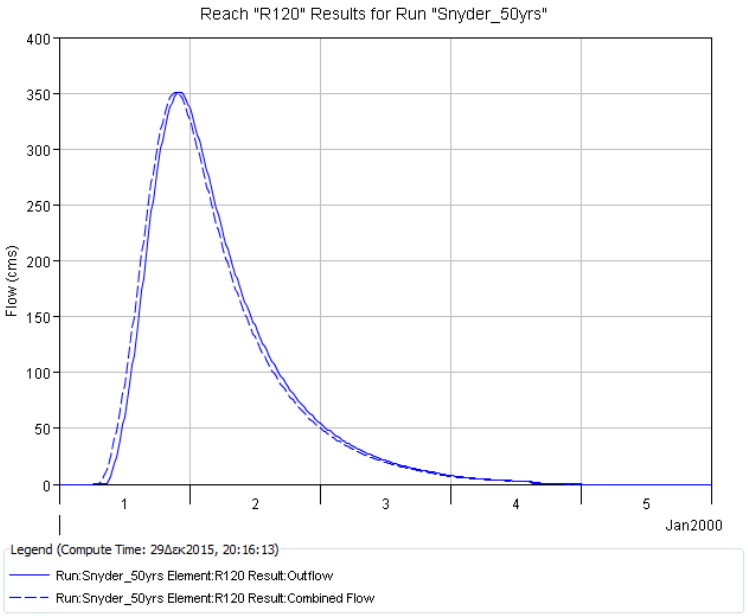

Figure 20. Final design hydrograph with Snyder method used for Muscingum – Cunge route method for 50 years flood period of Titarisios River, Thessaly.

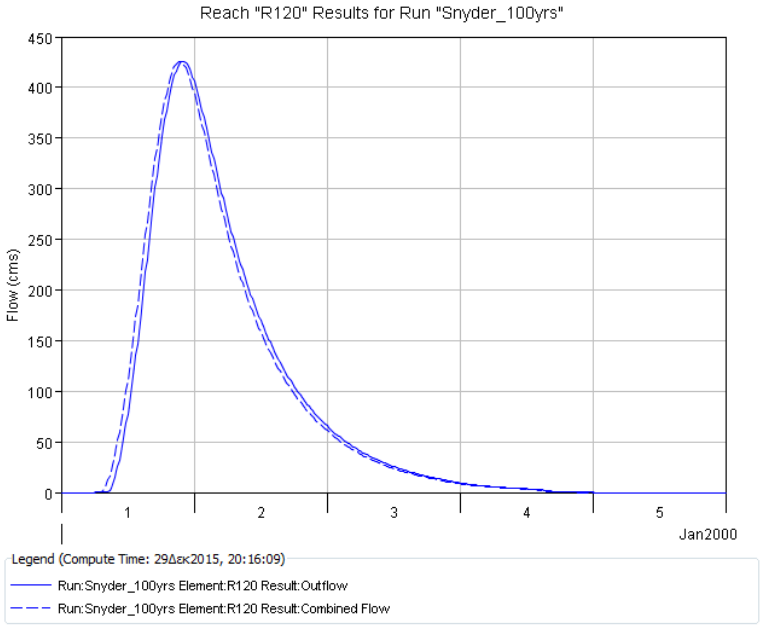

Figure 21. Final design hydrograph with Snyder method used for Muscingum – Cunge route method for 100 years flood period of Titarisios River, Thessaly.

Institutional Repository - Library & Information Centre - University of Thessaly
20/05/2024 06:18:41 EEST - 3.23.102.234

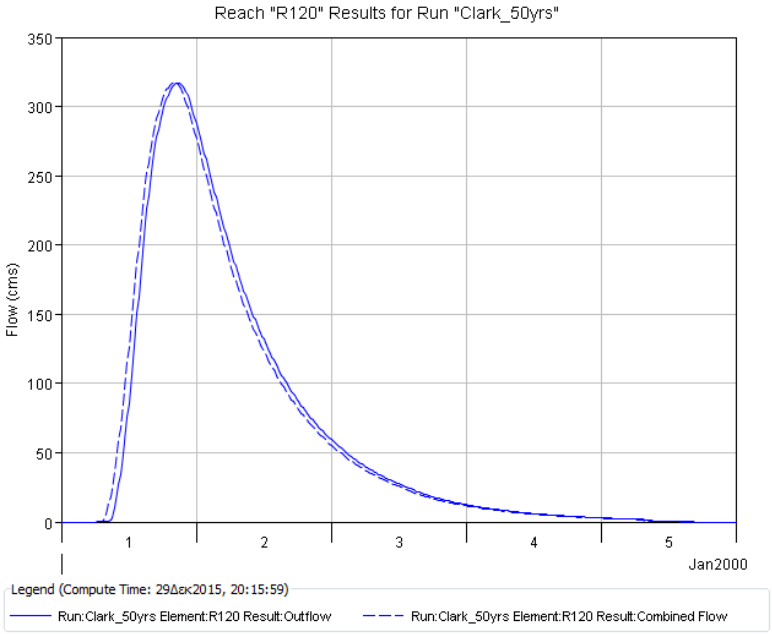

Figure 22. Final design hydrograph with Clark method used for Muscingum – Cunge route method for 50 years flood period of Titarisios River, Thessaly.

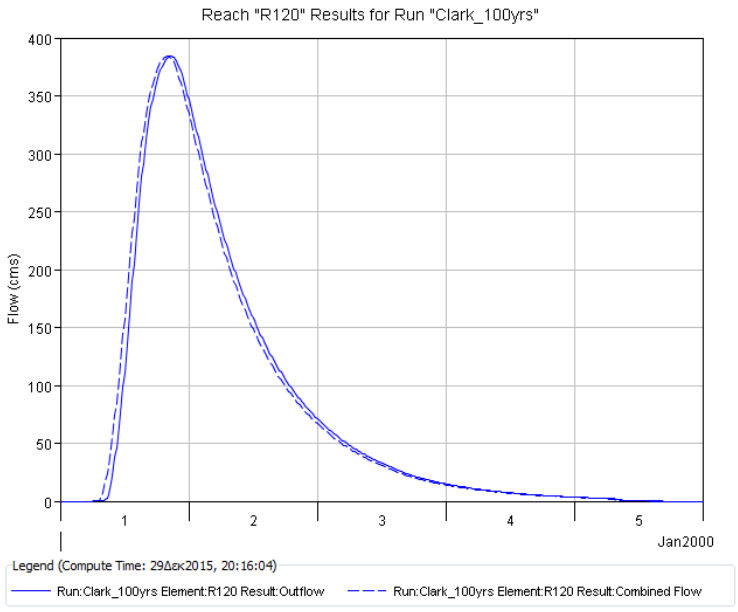

Figure 23. Final design hydrograph with Clark method used for Muscingum – Cunge route method for 100 years flood period of Titarisios River, Thessaly.

Institutional Repository - Library & Information Centre - University of Thessaly
20/05/2024 06:18:41 EEST - 3.23.102.234

Table 9. Peak discharge and discharge volume estimated in HEC-HMS with the three transform methods

	Flood period			
	50 yrs		100 yrs	
	Peak discharge (m3/sec)	Discharge volume (1000 m3)	Peak discharge (m3/sec)	Discharge volume (1000 m3)
Transform method				
SCS	771.1	27457.1	938.7	33275
Snyder	351	27454	425.6	33268.8
Clark	316.8	27454.5	384	33269.4

SCS method is based upon averages of Unit Hydrographs (UH) derived from gaged rainfall and runoff for a large number of small agricultural watersheds throughout the US. Because, of the geomorphology of Titarisios River basin, and, also, because of the estimation of Curve Number (CN), that is taking soil characteristics into account, SCS method should be appropriate for the synthetic hydrograph. Moreover, SCS method gives the worst-design unit hydrograph. According to Paraskevas et al (2015), in their study, over an integrated hydrological simulation of Xirias river basin in Magnesia, the design flood hydrographs were computed through the simulation of the basin's hydrologic model for two return-periods and three methods for estimating direct runoff were applied, and, finally, SCS transform method was selected.

In our case study, the worst-design hydrograph (SCS transform method) will be used to perform one-dimensional (1D) and two-dimensional (2D) unsteady flow analysis, for Titarisios River Reach, with HEC-RAS simulation program, for 50 and 100 years flood period.

Institutional Repository - Library & Information Centre - University of Thessaly
20/05/2024 06:18:41 EEST - 3.23.102.234

3 RESULTS

3.1 Topography of Titarisios River Reach

As above, an accurate digital elevation model (DEM) is appropriate in order to achieve a good approach of the inundation extent. Global Mapper simulated contours with 1 meter interval from ASTER GDEM v2 Worldwide Elevation Data, in Greek Grid projection. In this more detailed DEM, River Reach (blue line), river banks (red line) and cross sections (green line) along the river were designed (Figure 24). Moreover, residential areas like Ampelonas, Rodia, etc, were considered as areas that cannot be inundated (black polygons).

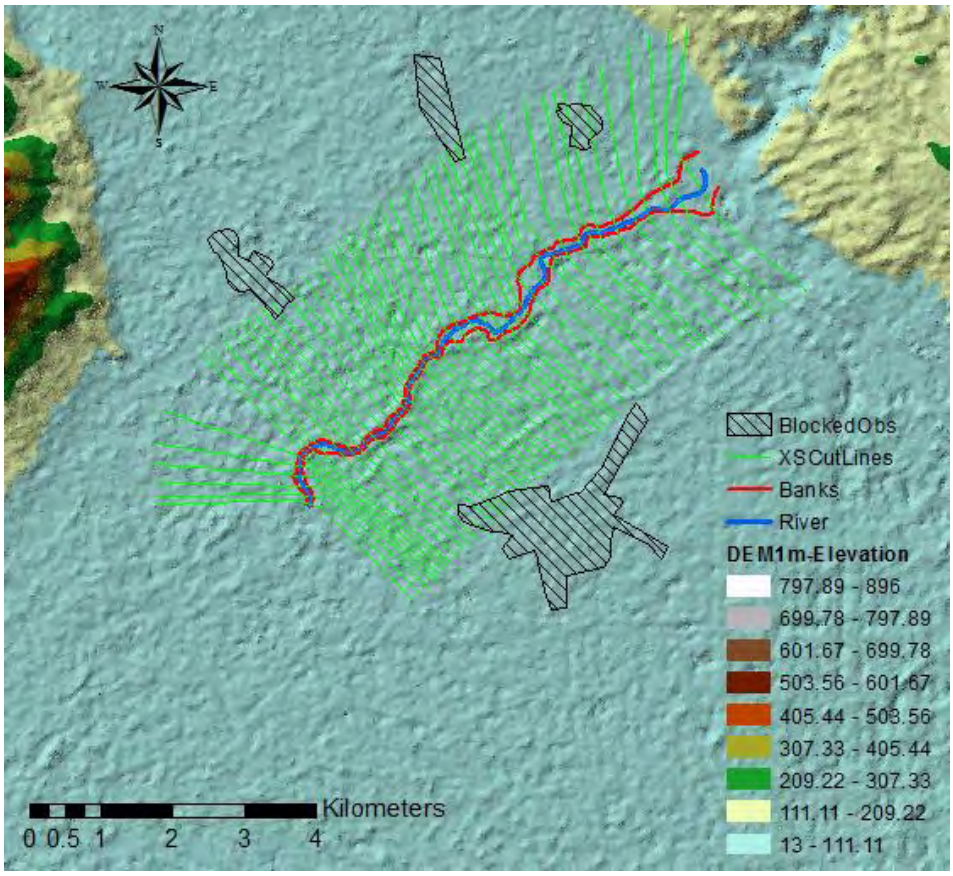

Figure 24. Representation of River Reach, Banks, Cross Sections and Blocked Areas designed with GeoRAS, in Arcmap Gis environment.

In Figure 25 it can be shown Manning's N values (Table A4, Appendix) stored for different land use types, derived by Corine Land Cover 2000. Discontinuous urban fabric, road and rail networks or mineral extraction sites will correspond to Manning's

Institutional Repository - Library & Information Centre - University of Thessaly
20/05/2024 06:18:41 EEST - 3.23.102.234

N values equal to 0.1. Respectively, water courses or beaches, dunes and sands will correspond to N values equal to 0.04. Non-irrigated areas or permanently irrigated areas have N values equal to 0.03 and 0.035. Those areas are close to the river banks. Cultivated areas will have N values equal to 0.05 and different type of forests 0.055 (Table 11). The Manning's N values are in accordance to Table 3-1 Manning's N values of the Reference Manual of HEC-RAS v4.1 (2010).

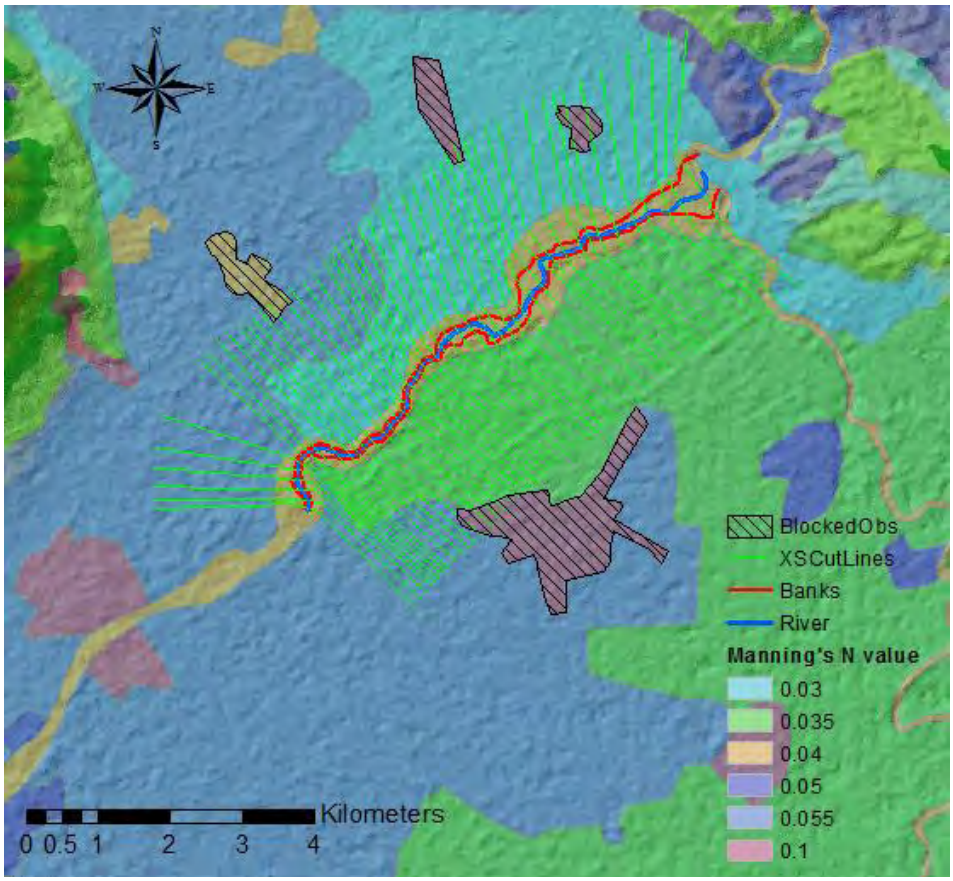

Figure 25. Manning's N Values estimated from Corine Land Cover 2000.

3.2 One-dimensional (1D) water surface profiles

HEC-RAS is capable of simulating one-dimensional unsteady flow through an open channel, Titarisios River Reach, in our case. The unsteady flow equation solver was adapted from Dr. Robert L. Barkau's UNET model (Barcau, 1992; HEC-RAS, 1997). Mixed flow regime water surface profiles will be calculated. Manning's n values will be composed in each cross section.

Institutional Repository - Library & Information Centre - University of Thessaly
20/05/2024 06:18:41 EEST - 3.23.102.234

3.2.1 Equations for basic profile calculations

Water surface profiles are computed from one cross section to the next by solving the Energy equation with an iterative procedure called the standard step method. The Energy equation is written as follows:

$$Y_2 + Z_2 + \frac{a_2 V_2^2}{2g} = Y_1 + Z_1 + \frac{a_1 V_1^2}{2g} + h_e \tag{38}$$

where Y_1, Y_2 is the elevation of the main channel inverts, Z_1, Z_2 is the depth of water at cross sections, V_1, V_2 are the average velocities (total discharge/total flow area), a_1, a_2 are the velocity weighting coefficients, g is the gravitional acceleration, h_e is the energy head loss. A diagram showing the terms of energy equation is shown in Figure 26.

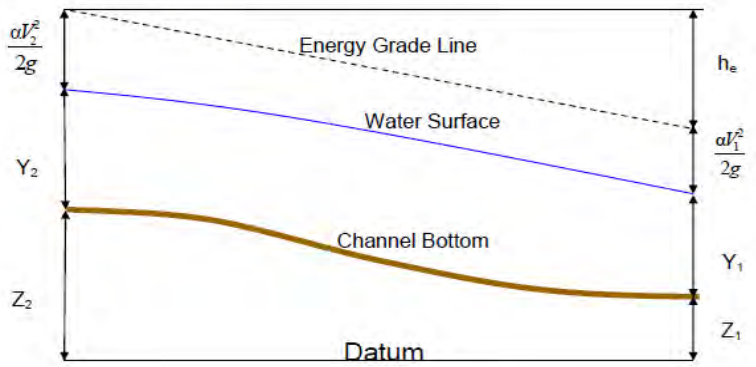

Figure 26. Representation of Terms in the Energy Equation.

The energy head loss (h_e) between two cross sections is comprised of friction losses and contraction or expansion losses. The equation for energy head loss is as follows:

$$h_e = L\overline{S_f} + c\left|\frac{a_2 V_2^2}{2g} - \frac{a_2 V_1^2}{2g}\right| \tag{39}$$

where L is discharge weighted reach length, S_f is representative friction between two slopes, c is expansion or contraction loss coefficient

The distance weighted reach length, L, is calculated as:

$$L = \frac{L_{lob}\overline{Q_{lob}} + L_{ch}\overline{Q_{ch}} + L_{rob}\overline{Q_{rob}}}{\overline{Q_{lob}} + \overline{Q_{rob}} + \overline{Q_{ch}}} \tag{40}$$

where L_{lob}, L_{rob}, L_c are the cross section reach lengths for flow in the left overbank, main channel, and right overbank, respectively, $\overline{Q_{lob}}$, $\overline{Q_{ch}}$, $\overline{Q_{rob}}$ is the arithmetic average

Institutional Repository - Library & Information Centre - University of Thessaly
20/05/2024 06:18:41 EEST - 3.23.102.234

of the flows between sections for left overbank, main channel, and right overbank respectively

3.2.2 Cross section subdivision for conveyance calculations

The determination of total conveyance and the velocity coefficient for a cross section requires that flow be subdivided into units for which the velocity is uniform distributed. The approach used in HEC-RAS is to subdivide flow in the overbank areas using the input cross section n-value break points (locations where n-values change) as the basis for subdivision. Conveyance is calculated within each subdivision from the following form of Manning's equation (based on English units):

$$Q = K S_f^{\frac{1}{2}} \tag{41}$$

$$K = \frac{1.486}{n} A R^{\frac{2}{3}} \tag{42}$$

where *K* is the conveyance for subdivision, *n* is the Manning's roughness coefficient for subdivision, *A* is flow area for subdivision, *R* is hydraulic radius for subdivision (area / wetted perimeter)

The program sums up all the incremental conveyances in the overbanks to obtain a conveyance for the left overbank and the right overbank. The main channel conveyance is normally computed as single conveyance element. The total conveyance for the cross section is obtained by summing the three subdivision conveyances (left, main channel, and right).

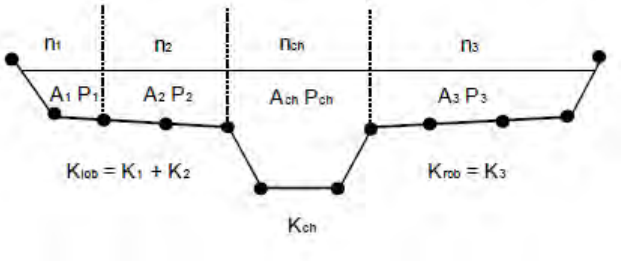

Figure 27. HEC-RAS default conveyance subdivision method.

3.2.3 Composite Manning's for the main channel

Flow in the main channel is not subdivided, except when the roughness coefficient is changed within the channel area. HEC-RAS tests the applicability of subdivision of roughness within the main channel portion of a cross section, and if it is not applicable the program will compute a single composite n value for the entire main channel. The program determines if the main channel portion of the cross section can be subdivided or if a composite main channel n value will be utilized as:

Institutional Repository - Library & Information Centre - University of Thessaly
20/05/2024 06:18:41 EEST - 3.23.102.234

$$n_c = \left[\frac{\sum_{i=1}^{N} \left(P_i n_i^{1.5} \right)}{P} \right]^{2/3} \quad (43)$$

where n_c is composite or equivalent coefficient of roughness, P is wetted perimeter of entire main channel, P_i is wetted perimeter of subdivision I, n_i is coefficient of roughness for subdivision

3.2.4 Evaluation of mean kinetic energy head

Because the HEC-RAS software is one-dimensional water surface profiles program, only a single water surface and therefore a single mean energy are computed at each cross section. For a given water surface elevation, the mean energy is obtained by computing a flow weighted energy from three subsections of a cross section (left overbank, main channel and a right overbank). Figure 28**,** below, shows how the mean energy would be obtained for a cross section with a main channel and a right overbank (no left overbank area).

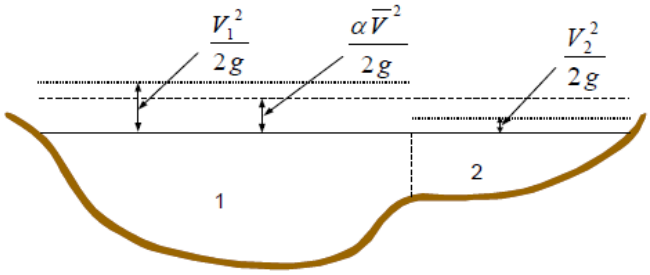

Figure 28. Example of how mean energy is obtained.

To compute the mean kinetic energy is necessary to obtain the velocity head weighting coefficient alpha. It is computed as follows:

$$a \frac{\overline{V^2}}{2g} = \frac{Q_1 \left(\frac{V_1^2}{2g} \right) + Q_2 \left(\frac{V_2^2}{2g} \right)}{Q_1 + Q_2} \quad (44)$$

Institutional Repository - Library & Information Centre - University of Thessaly
20/05/2024 06:18:41 EEST - 3.23.102.234

$$a = \frac{2g\left[Q_1\left(\frac{V_1^2}{2g}\right) + Q_2\left(\frac{V_2^2}{2g}\right)\right]}{(Q_1 + Q_2)\overline{V^2}} \tag{45}$$

$$a = \frac{Q_1 V_1^2 + Q_2 V_2^2}{(Q_1 + Q_2)\overline{V^2}} \tag{46}$$

In general:

$$a = \frac{Q_1 V_1^2 + Q_2 V_2^2 + ... + Q_N V_N^2}{Q\overline{V^2}} \tag{47}$$

The velocity coefficient, a, is computed based on the conveyance in the three flow elements: left overbank, right overbank and channel. It can be written in terms of conveyance and area as in the following equation:

$$a = \frac{(A_t)^2\left[\frac{(K_{lob})^3}{(A_{lob})^2} + \frac{(K_{ch})^3}{(A_{ch})^2} + \frac{(K_{rob})^3}{(A_{rob})^2}\right]}{(K_t)^3} \tag{48}$$

where A_t is total flow area of cross section, A_{lob}, A_{ch}, A_{rob} are flow areas of left overbank, main channel and right overbank, respectively, K_t is total conveyance of cross section, K_{lob}, K_{ch}, K_{rob} are conveyances of left overbank, main channel and right overbank, respectively

3.2.5 Friction loss equation

Friction loss is evaluated in HEC-RAS as the product of $\overline{S_f}$ and L (see Equation 39), where $\overline{S_f}$ is the representative friction slope, for a reach, and L is defined by Equation 40. The friction slope (slope of the energy gradeline) at each cross section is computed from Manning's equation as follows:

$$\overline{S_f} = \left(\frac{Q}{K}\right)^2 \tag{49}$$

3.2.6 Contraction and expansion loss evaluation

Contraction and expansion losses in HEC-RAS are evaluated by the following equation:

Institutional Repository - Library & Information Centre - University of Thessaly
20/05/2024 06:18:41 EEST - 3.23.102.234

$$h_0 = c \left| \frac{a_1 V_1^2}{2g} + \frac{a_2 V_2^2}{2g} \right| \quad (50)$$

where c is the contraction and expansion coefficient

The program assumes that a contraction is occurring whenever the velocity head downstream is greater than the velocity head upstream. Likewise, when the velocity head upstream is greater than the velocity downstream, the program assumes that a flow expansion is occurring.

In our case study, contraction coefficient is set equal to 0.1 and expansion coefficient equal to 0.3.

3.2.7 Unsteady flow equation

The hydraulic model, under unsteady flow, solves the continuity equation. Conservation of mass for a control volume states, that the net rate of flow into the volume be equal to the rate of change of storage inside the volume. The rate of inflow to the control volume may be written as:

$$Q - \frac{\partial Q}{\partial x} \frac{\Delta x}{2} \quad (51)$$

the rate of outflow as:

$$Q + \frac{\partial Q}{\partial x} \frac{\Delta x}{2} \quad (52)$$

and, the rate of change in storage as:

$$\frac{\partial A_T}{\partial t} \Delta x \quad (53)$$

Assuming that Δx is small, the change in mass in the control volume is equal to:

$$\rho \frac{\partial A_T}{\partial t} \Delta x - \rho \left[\left(Q - \frac{\partial Q}{\partial x} \frac{\Delta x}{2} \right) - \left(Q + \frac{\partial Q}{\partial x} \frac{\Delta x}{2} \right) + Q_L \right] \quad (54)$$

where Q_L is the lateral flow entering the control volume and ρ is the fluid density

Simplifying and divided through ρΔx yields the final form of the continuity equation:

$$\frac{\partial A_T}{\partial t} + \frac{\partial Q}{\partial x} - q_l = 0 \quad (55)$$

where A_T is the flow area of cross section, t is the time, Q is the flow entering the control volume, x is the distance along the channel flow and q_l is the lateral inflow per unit length

Institutional Repository - Library & Information Centre - University of Thessaly
20/05/2024 06:18:41 EEST - 3.23.102.234

With the additional storage term, the continuity equation is equal to:

$$\frac{\partial A_T}{\partial t} + \frac{\partial S}{\partial t} + \frac{\partial Q}{\partial x} - q_l = 0 \tag{56}$$

where S is the storage from non-conveying portions of cross sections

Conservation of momentum is expressed by Newton's law as:

$$\sum F_x = \frac{dM}{dt} \tag{57}$$

Conservation of momentum for a control volume, states that, the net rate of momentum entering the volume (momentum flux) plus the sum of external forces acting on the volume be equal to the rate of accumulation of momentum. This is a vector equation applied in x-direction. The momentum flux (MV) is the fluid mass times the velocity vector in the direction of flow. The forces will be considered as pressure, gravity, and boundary drag, or friction force. Momentum flux is denoted as the flux entering the control volume, written as:

$$\rho\left[QV - \frac{\partial QV}{\partial x}\frac{\Delta x}{2}\right] \tag{58}$$

and the flux leaving the volume may be written as:

$$\rho\left[QV + \frac{\partial QV}{\partial x}\frac{\Delta x}{2}\right] \tag{59}$$

Therefore, the net rate of momentum (momentum flux) entering the control volume is:

$$-\rho\frac{\partial QV}{\partial x}\Delta x \tag{60}$$

Since the momentum of the fluid in the control volume is ρΔx, the rate of accumulation of momentum may be written as:

$$\frac{\partial}{\partial t}\left(\rho Q\Delta x\right) = \rho\Delta x\frac{\partial Q}{\partial t} \tag{61}$$

Restating the principle of conservation of momentum will have that the net rate of momentum (momentum flux) entering the volume (Equation 60) plus the sum of all external forces acting on the volume is equal to the rate of accumulation of momentum (Equation 61). Hence:

$$\rho\Delta x\frac{\partial Q}{\partial t} = -\rho\frac{\partial QV}{\partial x}\Delta x - \rho gA\frac{\partial h}{\partial x}\Delta x - \rho gA\frac{\partial z_0}{\partial x}\Delta x - \rho gAS_f\Delta x \tag{62}$$

Institutional Repository - Library & Information Centre - University of Thessaly
20/05/2024 06:18:41 EEST - 3.23.102.234

The elevation of the water surface, z, is equal to z_0+h. Therefore:

$$\frac{\partial z}{\partial x} = \frac{\partial h}{\partial x} + \frac{\partial z_0}{\partial x} \tag{63}$$

where $\frac{\partial z}{\partial x}$ is the water surface slope

Substituting (Equation 63) into (Equation 62), dividing through by ρΔx and moving all terms to the left, yields the final form of the momentum equation:

$$\frac{\partial Q}{\partial t} + \frac{\partial QV}{\partial x} + gA\left(\frac{\partial z}{\partial x} + S_f\right) = 0 \tag{64}$$

where *Q* is the flow, *t* is the time, *x* is the distance along the channel flow, *V* is the velocity along x direction, *z* is the water surface elevation, *A* is the flow area of the cross sections, *g* is the acceleration of gravity, S_f is the friction slope

When the river is rising, water moves laterally away from the channel inundating the floodplain. As the depth increases, the floodplain begins to convey water downstream generally along a shorter path than that of the main channel. When the river stage is falling, water moves towards the channel from the overbank supplementing the flow in the main channel.

The most successful and accepted procedure for solving the one-dimensional (1D) unsteady flow equations is the four-point implicit scheme, known as box scheme (Figure 29). Under this scheme, space derivatives and function values are evaluated at an interior point (n+θ) Δt. Thus, values at (n+1) Δt enter into all terms in the equations. A system of simultaneous equations results. This is important, because it allows information from the entire reach, to influence solution at any point. Finite difference equations are linearized in HEC-RAS, a technique developed by Liggett and Cunge (1975) and Chen (1973). Various time and distance intervals were applied in order the one-dimensional model acquire accuracy and stability of the solution.

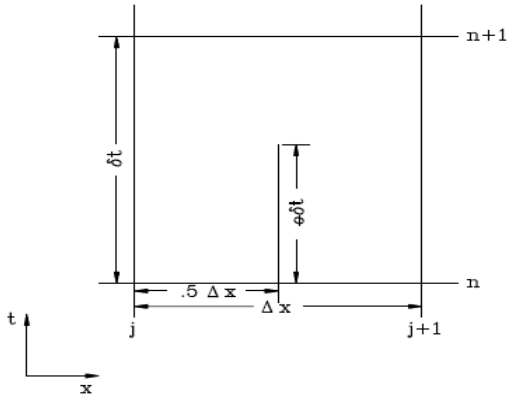

Figure 29. Typical finite difference cell.

Institutional Repository - Library & Information Centre - University of Thessaly
20/05/2024 06:18:41 EEST - 3.23.102.234

For Titarisios River Reach, there are N computational nodes which bound N-1 finite difference cells. From these cells 2N-2 finite difference equations can be developed. Because there are 2N unknowns (ΔQ and dz for each node), two additional equations are needed. These equations are provided by the boundary conditions, which for mixed flow are required at the upstream and downstream ends. For the upstream boundary condition we entered the worst designed flow hydrograph of discharge versus time, with data time interval equal to 15 minutes, derived with HEC-HMS (SCS transform method), for 50 and 100 years flood period, respectively. For downstream boundary conditions, normal depth equal to 0.0014 was used, which is the slope of the two last cross-sections, at the end of the Titarisios River Reach. Here, Manning's equation is used (Equation 41), where friction slope produces a stage considered to be normal depth if uniform flow conditions existed.

In addition to boundary conditions, it is required to establish the initial conditions (flow and stage) at all nodes in the system at the beginning of the simulation. If flow data is entered, then the program computes water surface elevations by performing a steady flow backwater analysis. Initial conditions in our study is 12 m3/sec for 50years flood period, and 18 m3/sec for 100 years flood period, respectively.

Unsteady flow analysis was prosecuted with computation interval equal to 5 sec, Hydrograph output interval every 5 minutes, detailed output interval equal to 1 hour. Mapping output interval, for inundation mapping, is every 5 minutes. Total time of simulation is set 24.75 hours (starts at 01DEC2015, 24:00, and ends at 03DEC2015, 00:45), which is, also, the duration of the flood hydrograph, entered as upstream boundary condition.

Water surface calculation tolerance is 0.003, with max error in water surface solution to be 30 meters. For the simulation, 20 maximum warm up time steps were entered, and, also, 20 maximum number of iterations. Theta (implicit weighting factor) entered equal to 1, as well as, theta for warm up equal to 1.

In HEC-RAS environment, we can represent the characteristics (river reach, banks, cross sections, block object, Manning's n values) of Titarisios River Reach (Figure 30).

Institutional Repository - Library & Information Centre - University of Thessaly
20/05/2024 06:18:41 EEST - 3.23.102.234

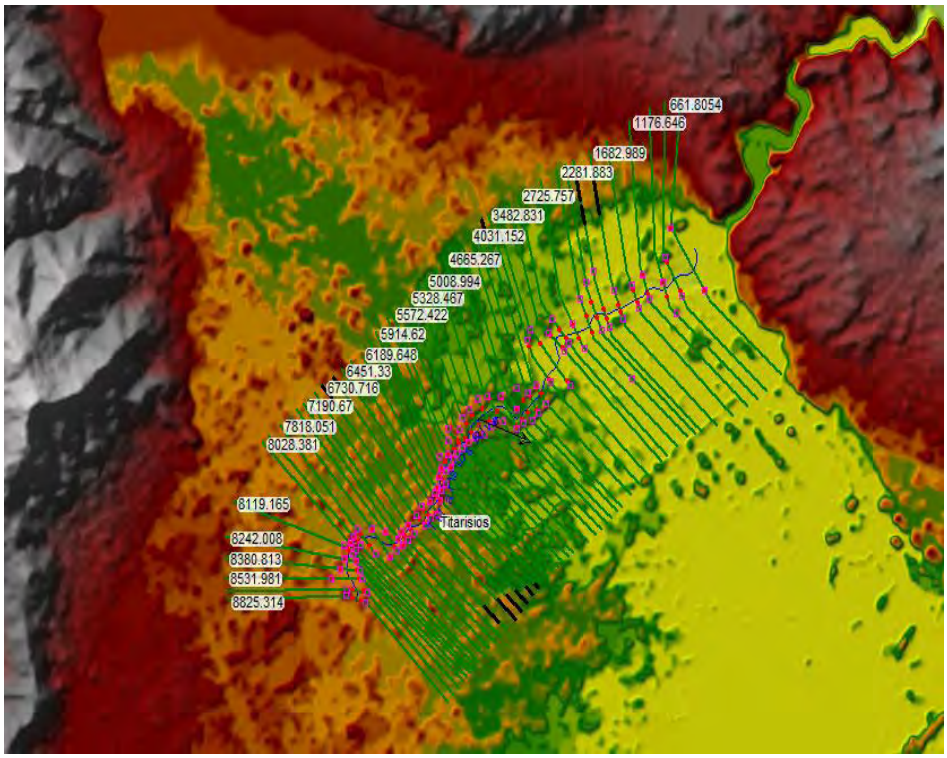

Figure 30. Representation of Titarisios River Reach in HEC-RAS environment.

One-dimensional (1D) unsteady flow analysis, with mixed flow regime, of 50 and 100 years flood period, results to water surface profile (Figure 31), with elevation versus main channel distance and velocity profile (Figure 32), with velocity versus main channel distance.

Institutional Repository - Library & Information Centre - University of Thessaly
20/05/2024 06:18:41 EEST - 3.23.102.234

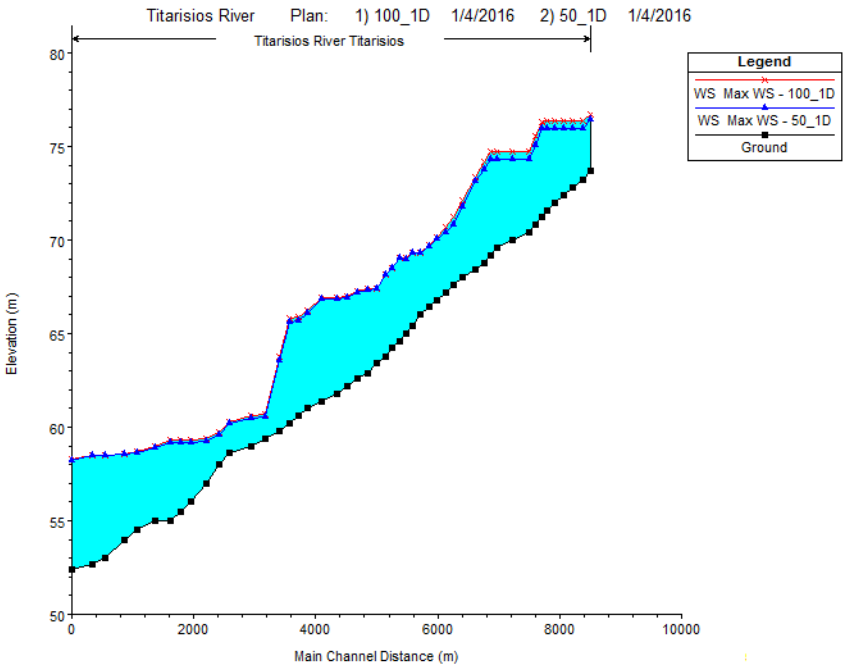

Figure 31. Water surface profiles of one-dimensional (1D) simulation for 50 and 100 years flood period.

As expected, water surface elevation is higher for 100 years flood period, than for 50 years flood period. Similarly, maximum velocity for 100 years flood period is larger than for 50 years flood period. Judging from the Figures, but, also, from results in Table A5 (Appendix), the simulation is quite smooth, since Froude number is normal for a mixed flow regime, except for cross-sections 7929.131 (6.25 m/sec and 5.87 m/sec, for 50 and 100 years, respectively) and 6189.648 (8.76 m/sec and 9.00 m/sec, for 50 and 100 years, respectively), where water surface elevations and velocities increase. If we look at the energy grade (0.0156 and 0.0143), for the cross-section 7929.131 and (0.1536 and 0.1611) for the cross-section 6189.648, for 50 and 100 years respectively, we can conclude that in these cross-sections, slope changes, becomes steeper, and has as a result the water surface, but, mostly, the velocity to change.

Institutional Repository - Library & Information Centre - University of Thessaly
20/05/2024 06:18:41 EEST - 3.23.102.234

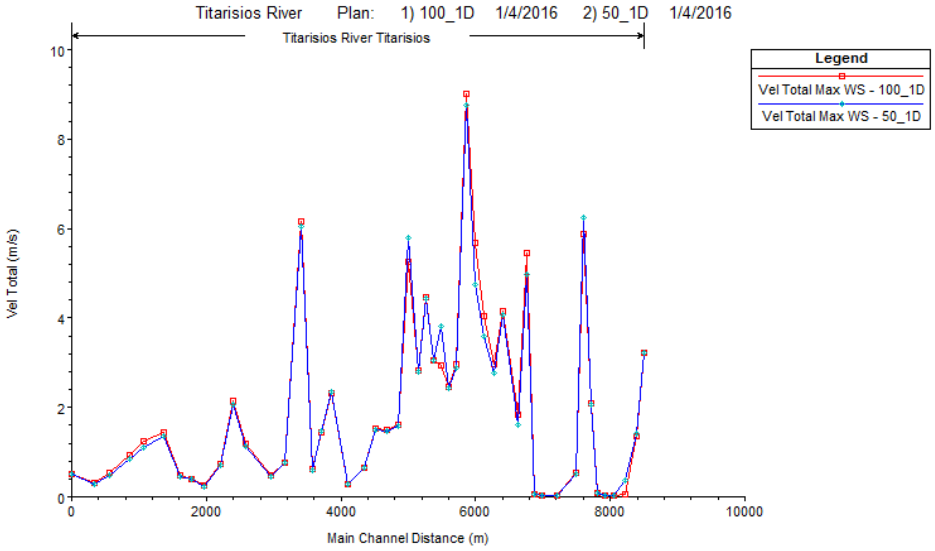

Figure 33. Velocity profiles of one-dimensional (1D) simulation for 50 and 100 years flood period.

Figures 33 and 34 present two different cross-sections, 8825.314 and 8531.981, the first to have adequate flow capacity, while the second to flood.

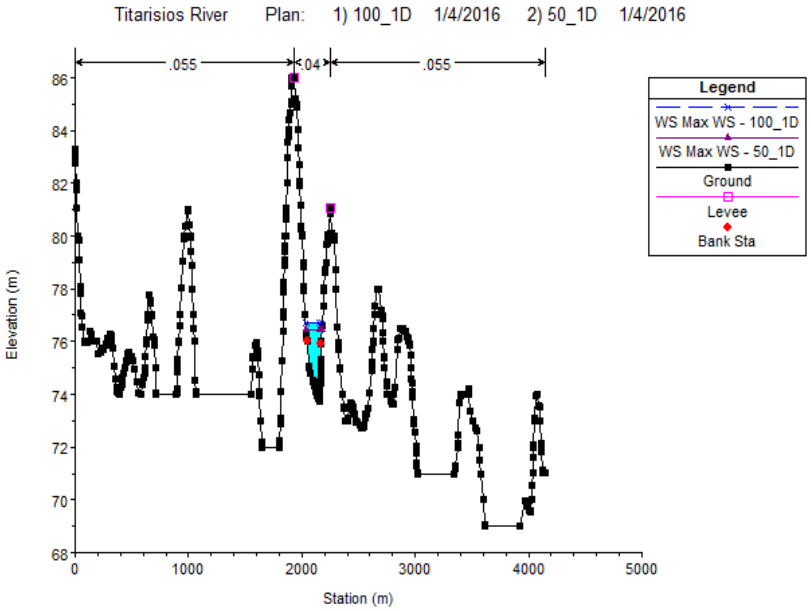

Figure 33. Cross section 8825.314 of one-dimensional (1D) simulation for 50 and 100 years flood period, without flooding.

Institutional Repository - Library & Information Centre - University of Thessaly
20/05/2024 06:18:41 EEST - 3.23.102.234

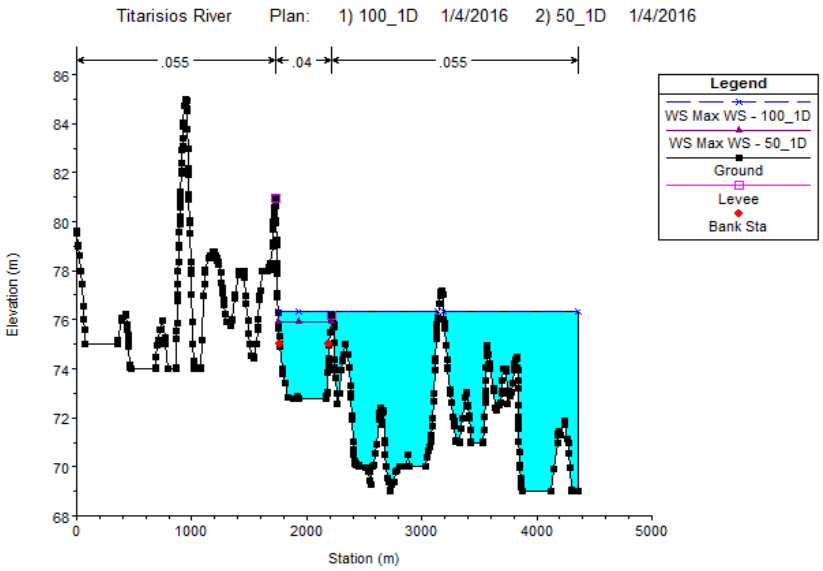

Figure 34. Cross section 8531.981 of one-dimensional (1D) simulation for 50 and 100 years flood period, with flooding.

The results of active flow area of the one-dimensional (1D) unsteady flow analysis, for 50 and 100 years flood period, are given in Table 10. The results of the simulations are shown in Table A5 (Appendix).

Table 10. Flow areas for 50 and 100 years flood period.

Flood period (yrs)	Area (km2)
50	0.09074604
100	0.11382272

It order to represent the full extent of inundation maps for one-dimensional (1D) flow analysis, larger cross sections should be designed. In our case, because the topography is quite flat, cross sections have been designed large enough to present the positions that will be inundated. The inundation maps of the one-dimensional (1D) unsteady flow analysis, for 50 and 100 years flood period, are presented in Figures 35 and 36, respectively, while in Figure 37, it can be seen the difference between 50 and 100 year flood period.

Institutional Repository - Library & Information Centre - University of Thessaly
20/05/2024 06:18:41 EEST - 3.23.102.234

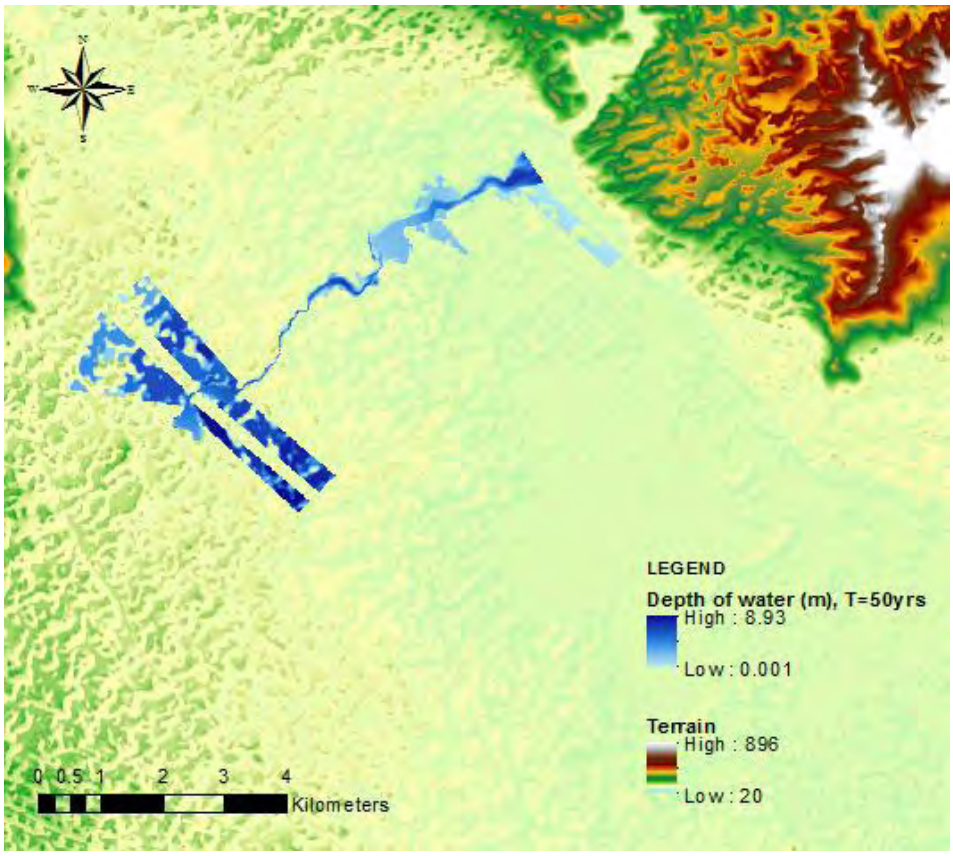

Figure 35. Inundation map of one-dimensional (1D) simulation, for 50 years flood period.

Institutional Repository - Library & Information Centre - University of Thessaly
20/05/2024 06:18:41 EEST - 3.23.102.234

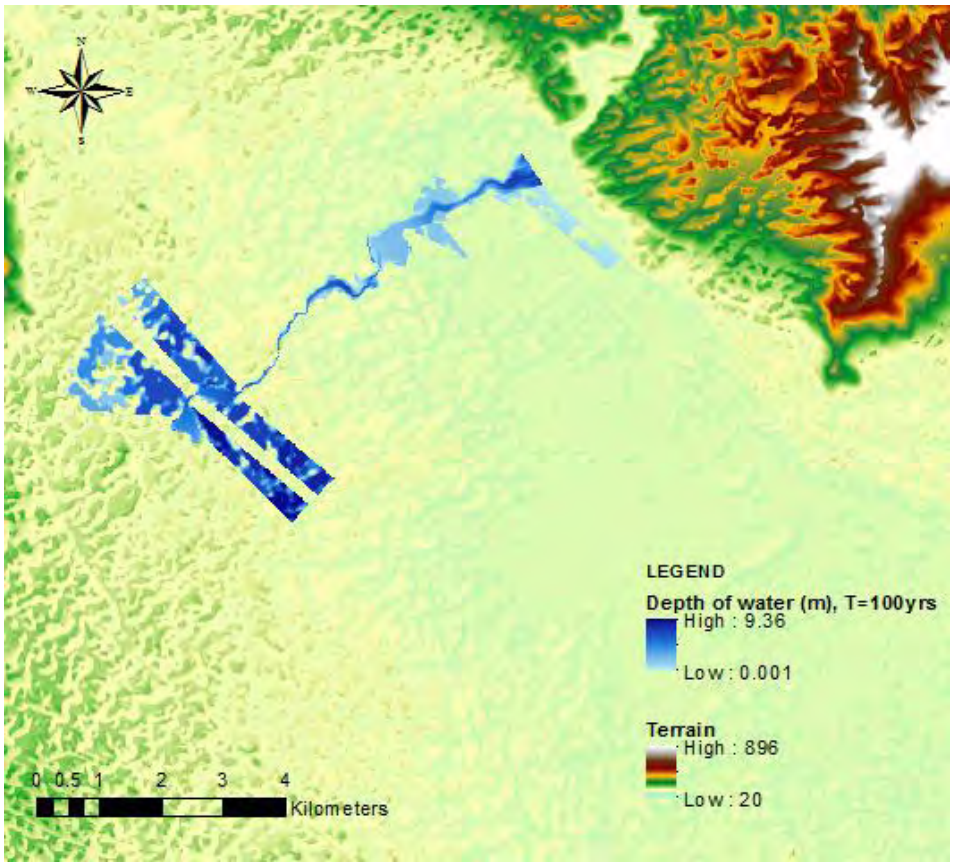

Figure 36. Inundation map of one-dimensional (1D) simulation, for 100 years flood period.

Institutional Repository - Library & Information Centre - University of Thessaly
20/05/2024 06:18:41 EEST - 3.23.102.234

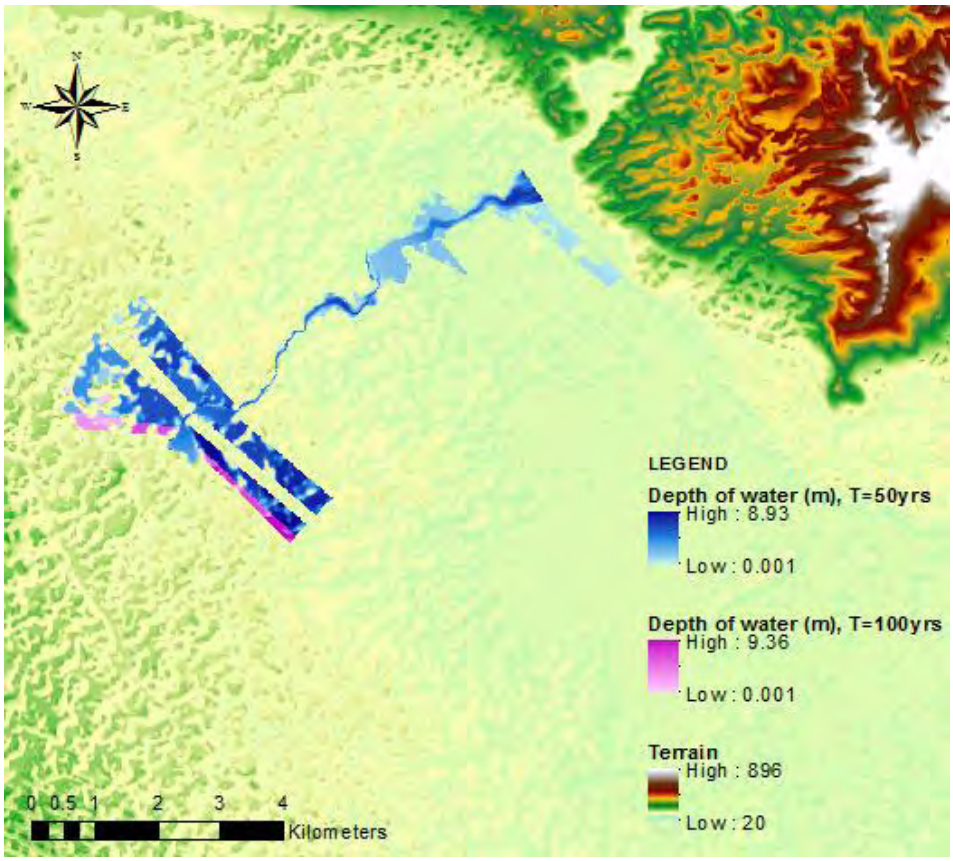

Figure 37. Inundation map of one-dimensional (1D) simulation for 50 and 100 years flood period.

3.3 Two-dimensional (2D) water surface profiles

The 2D area model for the two-dimensional unsteady flow analysis is built in terrain with 1 meter grid-cell resolution, with Greek Grid spatial reference projection. Because the terrain model is not so accurate in the channel region, we use a combined terrain that includes the initial terrain and a more detailed terrain of the channel. This can be created by the cross sections used in one-dimensional (1D) unsteady flow analysis. The combined terrain has exactly the same resolution, as the initial terrain (1 meter grid-cell).

For 2D modeling Finite Solution Scheme will be used by HEC-RAS. The program makes the computational mesh by following the Delaunay Triangulation technique, and then constructing a Voronoi diagram (Brunner, 2014) The unstructured computation mesh will have computation cell size equal to 100x100 meters and will consist of 8377 cells with maximum 8 sides in a computational cell. The statistics of the 2D computation mesh are given in Table 11 and the representation of the area is shown in

Institutional Repository - Library & Information Centre - University of Thessaly
20/05/2024 06:18:41 EEST - 3.23.102.234

Figure 38. Since the terrain and the water surface are small and they are not changing rapidly, cell size is appropriate for our study. The elevation-volume relationship is based on the detailed terrain data (1 meter grid), within each cell. This allow the use of larger computational sizes without losing too much of the details of the underlying terrain that govern the movement of the flow.

Table 11. Statistics of the 2D mesh with grid resolution 100x100m

	Area (m2)
Max cell	22276.39
Min cell	3230.01
Avg cell	10016.64

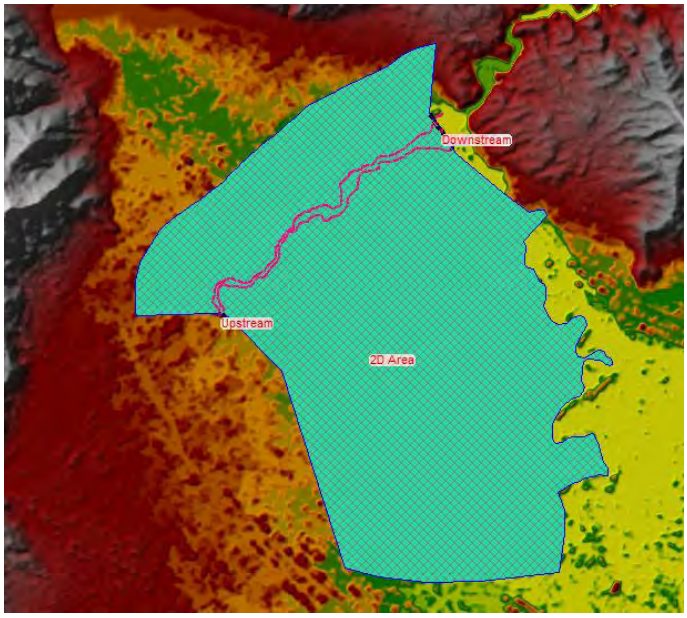

Figure 38. Two-dimensional (2D) area built by 100x100 meters grid-cells, representing upstream and downstream boundaries.

In addition to the design of the 2D area, it is necessary to add break lines along to the main river banks (Figure 39), in order to keep flow in the channel, until it gets high enough to overtop any high ground berm along the main channel.

Institutional Repository - Library & Information Centre - University of Thessaly
20/05/2024 06:18:41 EEST - 3.23.102.234

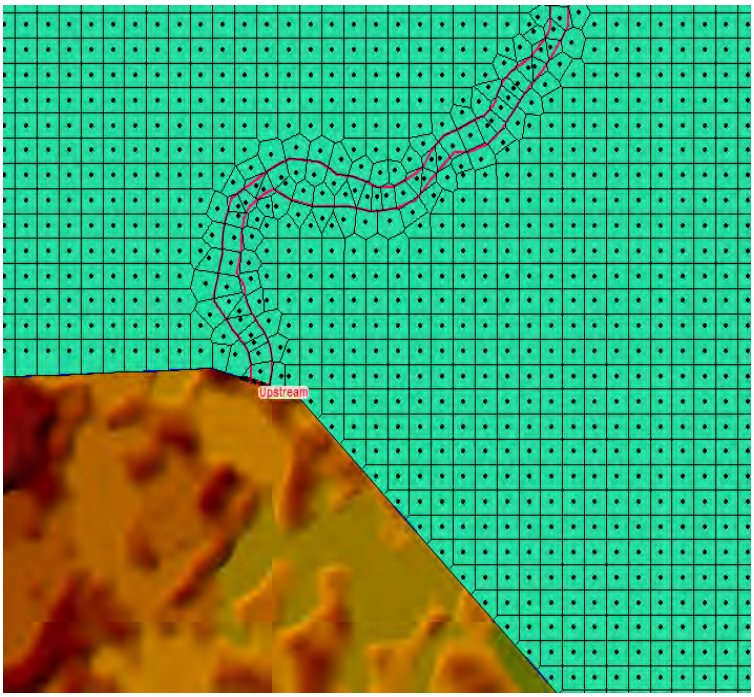

Figure 39. Detailed two-dimensional (2D) area built by 100x100 meters grid-cells, representing break lines (red lines).

A spatially varying land cover data set created in Arcmap Gis environment can be used in 2D unsteady flow analysis specifying Manning's n values for each land cover type. As in one-dimensional (1D) analysis, Corine Land Cover 2000 is used.

Figures 40 and 42 represent a 2D computational cell upstream (cell 8046), and downstream (cell 252) Titarisios River Reach, respectively. 2D computational mesh is pre-processed into an elevation volume for each cell, and a series of hydraulic property curves for each cell face (side of polygon), such as elevation versus face area, wetted perimeter, and roughness, as shown in Figures 41 and 43, corresponding to cell faces 8371 (upstream boundary) and 985 (downstream boundary). The hydraulic properties are derived from details on the underlying terrain used by the model.

Institutional Repository - Library & Information Centre - University of Thessaly
20/05/2024 06:18:41 EEST - 3.23.102.234

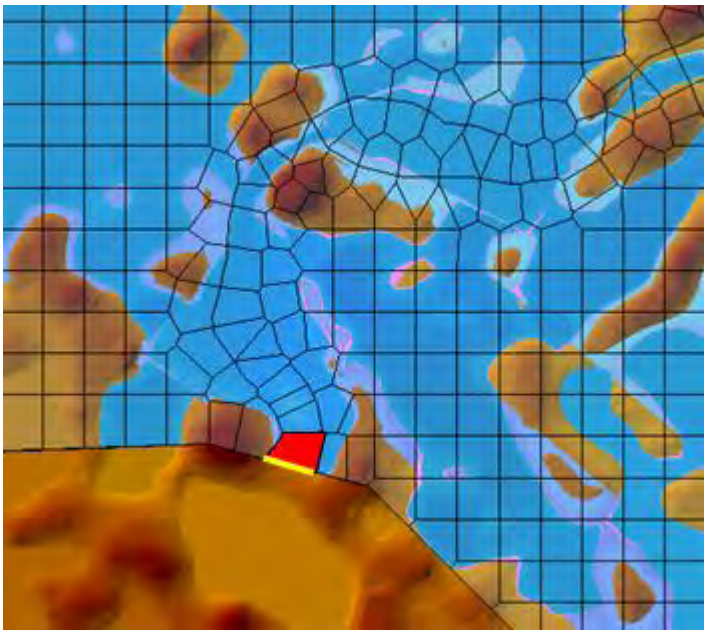

Figure 40. 2D computational cell (8046, red polygon) upstream Titarisios River Reach, including the upstream boundary cell face (8371, yellow line).

Institutional Repository - Library & Information Centre - University of Thessaly
20/05/2024 06:18:41 EEST - 3.23.102.234

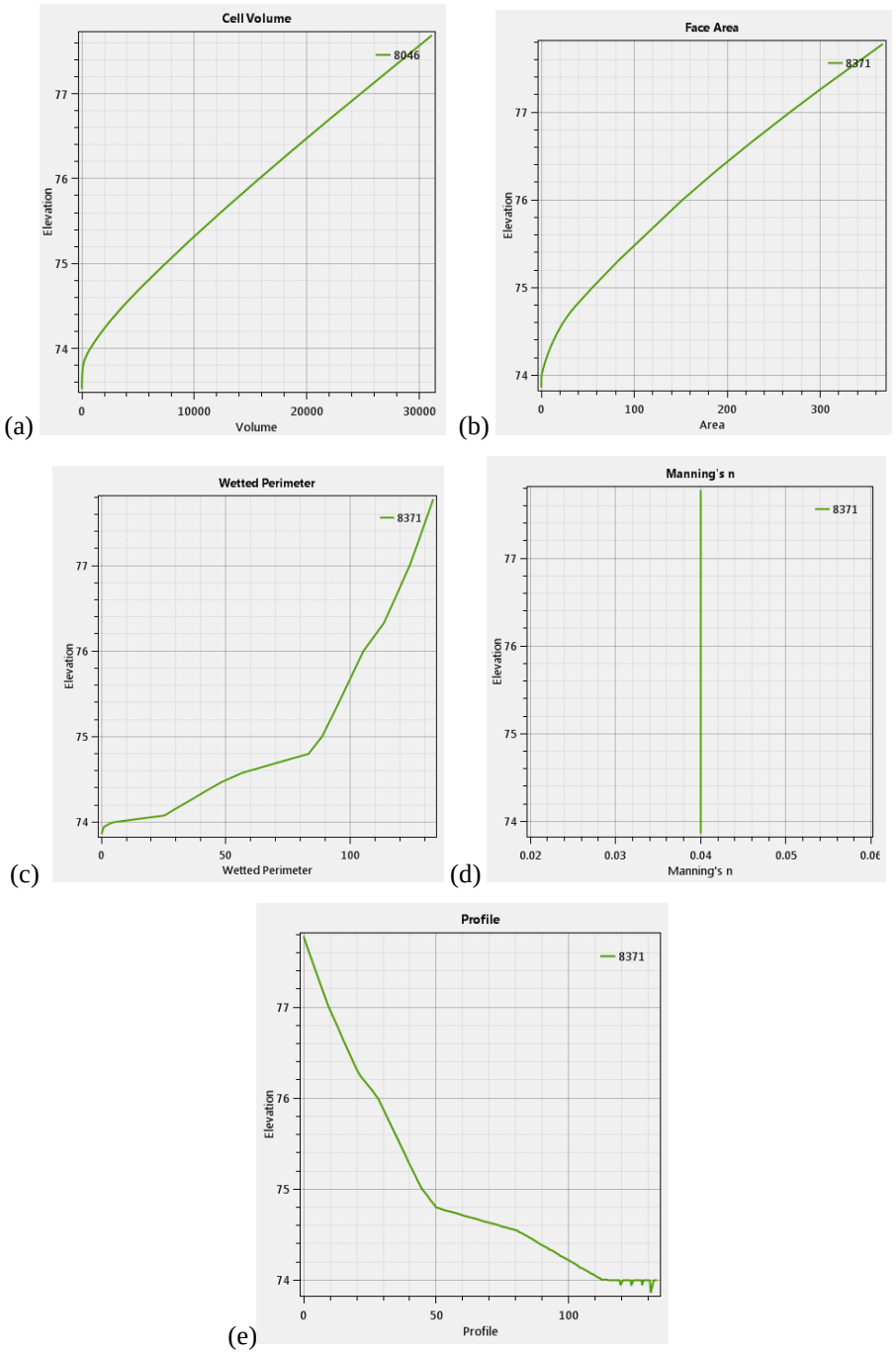

Figure 41 ((a), (b),(c), (d), (e)). Hydraulic properties of 2D computational cell (8046) and its cell face (8371) upstream Titarisios River Reach.

Institutional Repository - Library & Information Centre - University of Thessaly
20/05/2024 06:18:41 EEST - 3.23.102.234

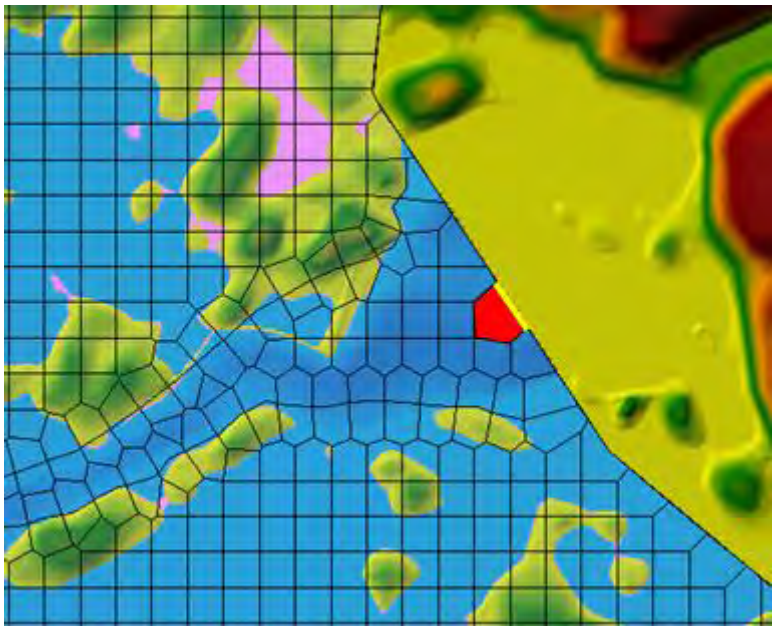

Figure 42. 2D computational cell (525, red polygon) downstream Titarisios River Reach, including the downstream boundary cell face (985, yellow line).

Institutional Repository - Library & Information Centre - University of Thessaly
20/05/2024 06:18:41 EEST - 3.23.102.234

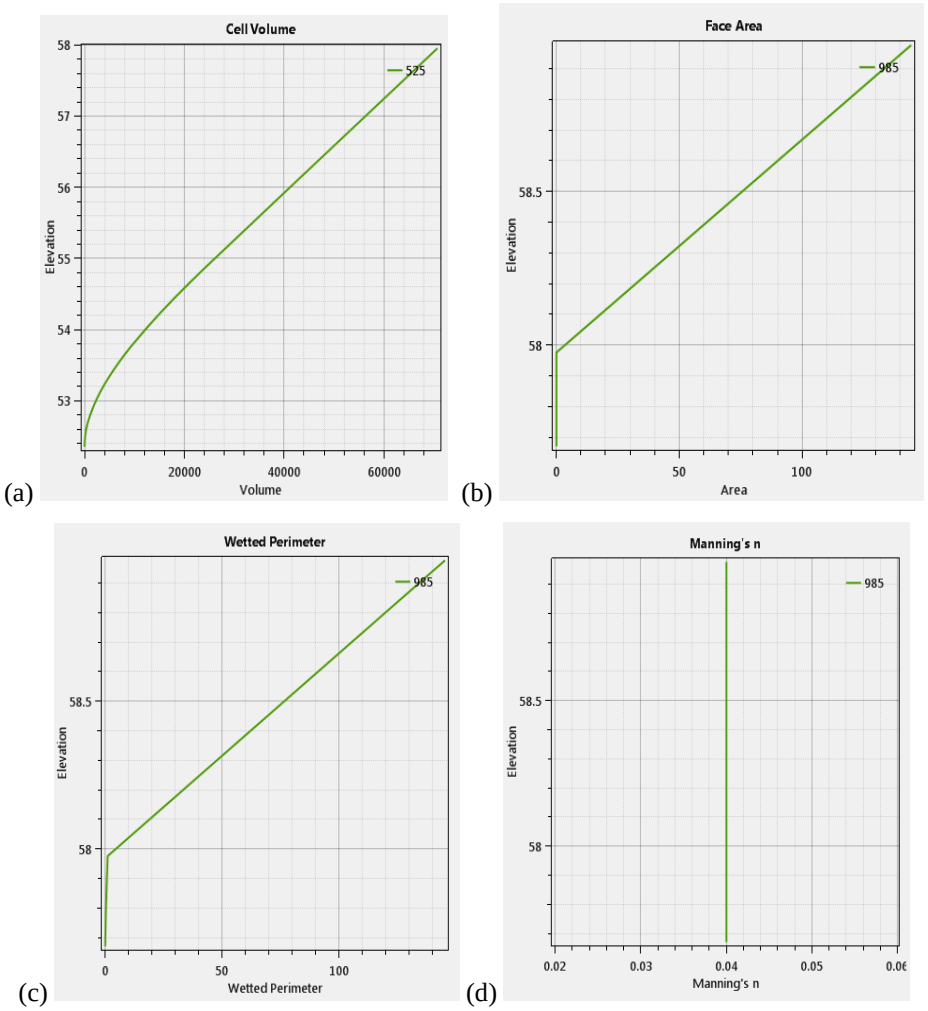

Figure 43 ((a), (b),(c), (d)). Hydraulic properties of 2D computational cell (525) and its cell face (985) downstream Titarisios River Reach.

3.3.1 Two-dimensional (2D) unsteady equation

Two-dimensional (2D) unsteady flow analysis will be performed with full momentum or Saint Venant equation. Although the program runs faster with 2D diffusion wave equations, and have more stability, we select 2D Saint Venant equation, because they result to smaller flood areas.

$$\frac{\partial Q}{\partial t}+\frac{\partial QV}{\partial x}+\frac{\partial QU}{\partial y}+gA\left(\frac{\partial z}{\partial x}+\frac{\partial z}{\partial y}+S_f\right)=0 \qquad (64)$$

Institutional Repository - Library & Information Centre - University of Thessaly
20/05/2024 06:18:41 EEST - 3.23.102.234

where Q is the flow, t is the time, x is the distance along the channel flow, y is the distance perpendicular to the flow, V is the velocity along x direction, U is the velocity along y direction, z is the water surface elevation, A is the flow area of the cross sections, g is the acceleration of gravity, S_f is the friction slope

As in one-dimensional (1D) flow analysis, 2D flow unsteady flow analysis is realized through an Implicit Finite Computational algorithm. The implicit solution algorithm allows for larger computational time steps than explicit methods. The Finite Volume Method provides an increment of improved stability and robustness over traditional finite difference and finite element techniques.

For Titarisios River Reach, there are N computational nodes which bound N-1 finite difference cells. From these cells 2N-2 finite difference equations can be developed. Because there are 2N unknowns (ΔQ and dz for each node), two additional equations are needed. These equations are provided by the boundary conditions, which for mixed flow are required at the upstream and downstream ends. For the upstream boundary condition we entered the worst designed flow hydrograph of discharge versus time, with data time interval equal to 15 minutes, derived with HEC-HMS (SCS transform method), for 50 and 100 years flood period, respectively. For downstream boundary conditions, normal depth equal to 0.0014 was used, which is the slope of the two last cross-sections, at the end of the Titarisios River Reach. Here, Manning's equation is used (Equation 41), where friction slope produces a stage considered to be normal depth if uniform flow conditions existed.

In addition to boundary conditions, it is required to establish the initial conditions (flow and stage) at all nodes in the system at the beginning of the simulation. If flow data is entered, then the program computes water surface elevations by performing a steady flow backwater analysis. As initial conditions, in two-dimensional (2D) simulation, water surface at the end of the reach, having been computed in one-dimensional (1D) at time step 00:00, is used, so as to keep all initial conditions similar. Thus, 2D flow areas will not start completely dry. Initial water surface is equal to 56.21 meters for 50years flood period, and equal to 56.60 meters for 100 years flood period, respectively.

As in one-dimensional model (1D), unsteady flow analysis for two-dimensional model (2D) was prosecuted with computation interval equal to 5 sec, Hydrograph output interval every 5 minutes, detailed output interval equal to 1 hour. Mapping output interval, for inundation mapping, is every 5 minutes. Total time of simulation is set 24.75 hours (starts at 01DEC2015, 24:00, and ends at 03DEC2015, 00:45), which is, also, the duration of the flood hydrograph, entered as upstream boundary condition.

For numerically stable and accurate solutions, a computational interval can be estimated as:

$$C = \frac{V\Delta \mathrm{T}}{\Delta \mathrm{X}} \le 1.0 \tag{66}$$

where C is the Courant number (maximum 3.00), V is the velocity of the flood wave (m/sec), ΔT is the computational time step (sec), ΔX is the average cell size (meters)

Water surface calculation tolerance is 0.01. For the simulation, we set, again, 20 maximum number of iterations. Initial conditions time was set 2 hours. Theta (implicit weighting factor) entered equal to 1, as well as, theta for warm up equal to 1.

Institutional Repository - Library & Information Centre - University of Thessaly
20/05/2024 06:18:41 EEST - 3.23.102.234

3.3.2 Velocity maps

In two-dimensional (2D) flow analysis, velocity can be computed at all locations, and can be, also, spatially interpolated between these locations. Figures 44 and 45 are presented for better understanding of the velocity flow field, in both magnitude and direction. The position is among the cross-sections 8380.813 and 7190.67 (Figure 30). As we can see, the differences between the two simulations at 02Dec2015, 15:00, for 50 and 100 years flood period, are very small, but, they still, exist. The larger are the arrows (black arrows), the bigger is the velocity.

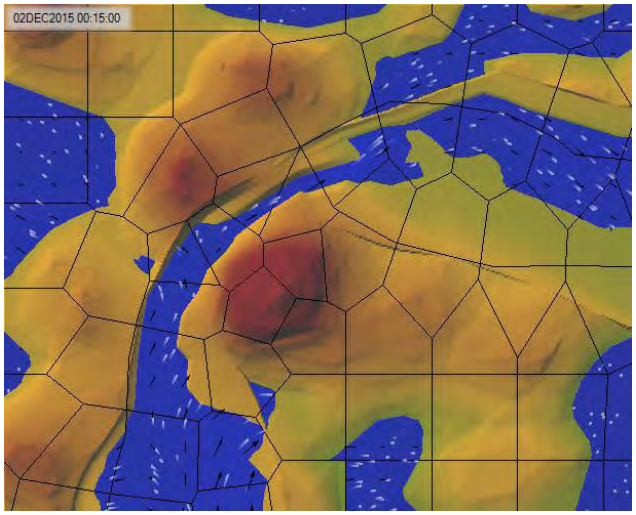

Figure 44. Velocity map of two-dimensional (2D) simulation, at 02Dec2015, 15:00, for 50 years flood period.

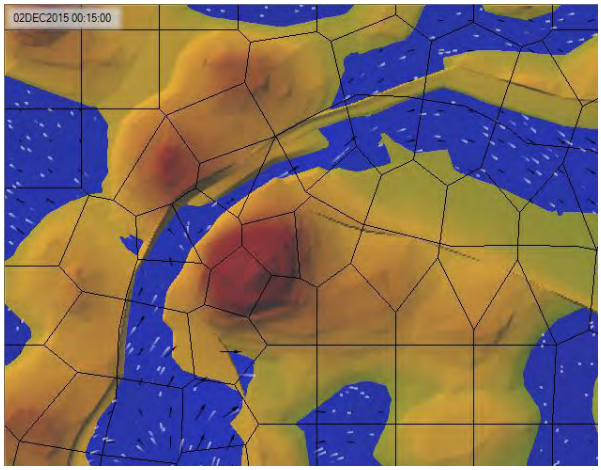

Figure 45. Velocity map of two-dimensional (2D) simulation, at 02Dec2015, 15:00, for 100 years flood period.

Institutional Repository - Library & Information Centre - University of Thessaly
20/05/2024 06:18:41 EEST - 3.23.102.234

3.3.3 Inundation maps based on 2D unsteady flow analysis

The inundation maps of the two-dimensional (2D) unsteady flow analysis, for 50 and 100 years flood period, are presented in Figures 46 and 47, respectively, while in Figure 46, the difference between 50 and 100 year flood period is shown.

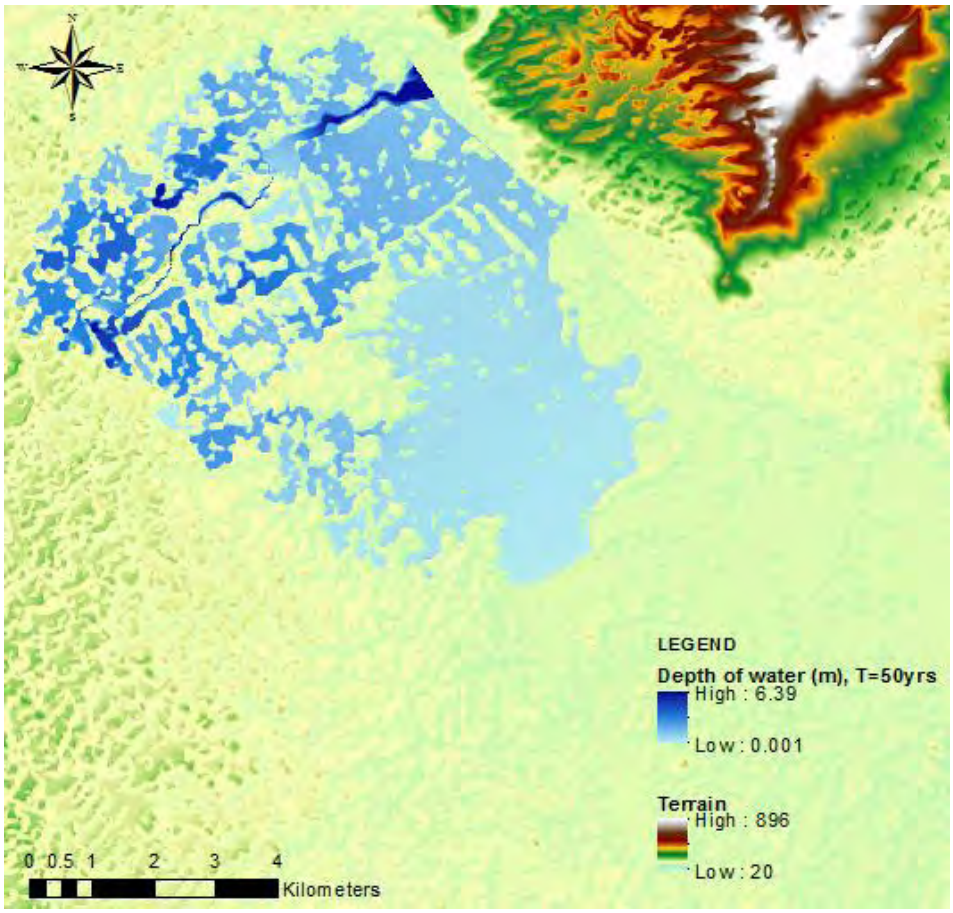

Figure 46. Inundation map of two-dimensional (2D) simulation, for 50 years flood period.

Institutional Repository - Library & Information Centre - University of Thessaly
20/05/2024 06:18:41 EEST - 3.23.102.234

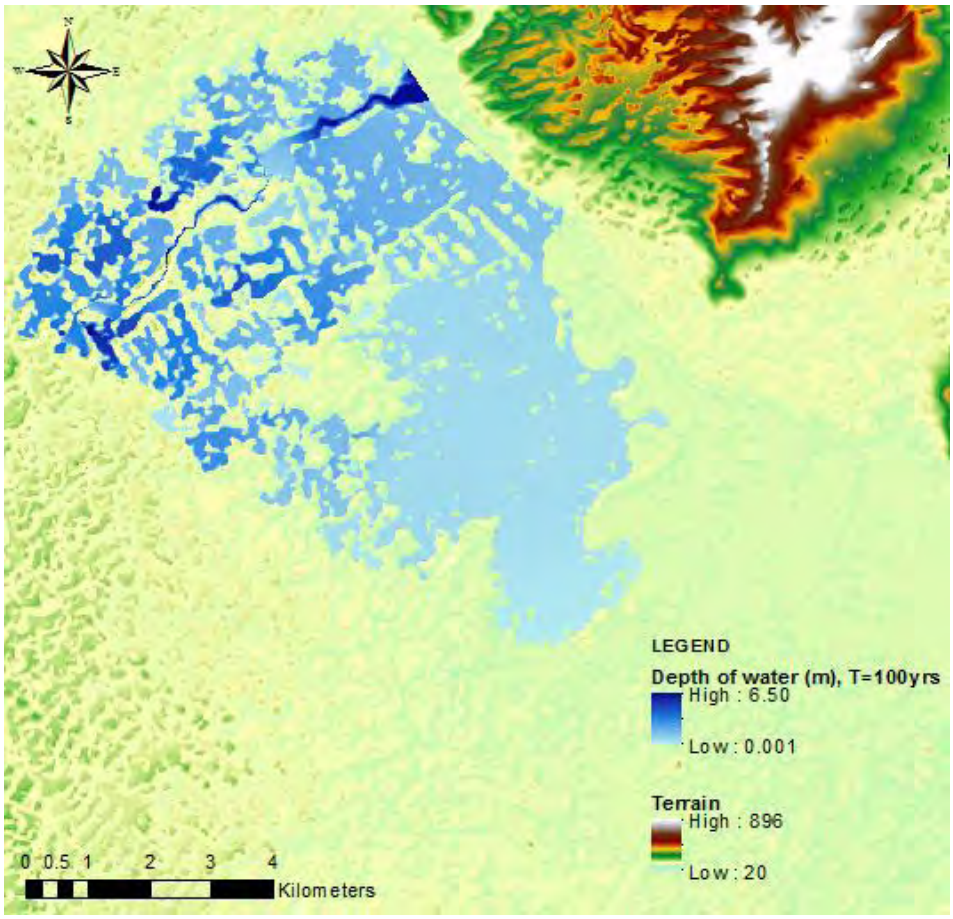

Figure 47. Inundation map of two-dimensional (2D) simulation, for 100 years flood period.

Institutional Repository - Library & Information Centre - University of Thessaly
20/05/2024 06:18:41 EEST - 3.23.102.234

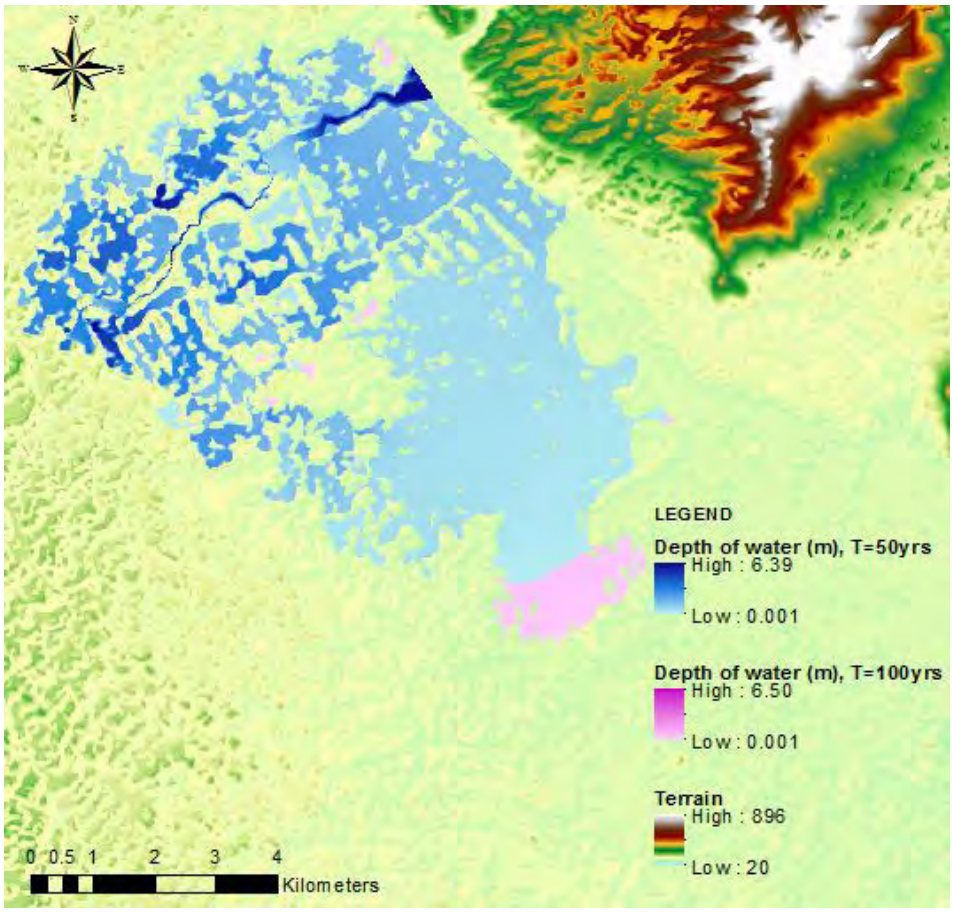

Figure 48. Inundation map of two-dimensional (2D) simulation for 50 and 100 years flood period.

3.4 Comparison of one-dimensional (1D) and two-dimensional (2D) unsteady flow analysis

One-dimensional (1D) as well as, two-dimensional unsteady flow analysis result in different inundation maps. As one can see from the above results, 2D analysis represents flood as it could take place (Figures 46 and 47), while one-dimensional (1D) unsteady flow analysis is incable of capturing the real extent of the inundated area (Figures 35 and 36).

Institutional Repository - Library & Information Centre - University of Thessaly
20/05/2024 06:18:41 EEST - 3.23.102.234

Table 12. Statistics of the 1-D and 2-D flood area

Flood period (yrs)	1D Flood Area (km2)	2D Flood Area (km2)
50	0.091	49.779
100	0.114	52.718
Difference (%)	25.430	5.903

Table 12 presents flood area for one-dimensional (1D) and two-dimensional (2D) unsteady flow analysis. As we can see by the differences (%), inundation area is increased when flow (flood period) is increased. The topography is quite flat, so the difference in flood area, it is expected for one-dimensional analysis to be quite large. (25%). On the opposite, when a flood area is steep, according to Giokas study (2009), which showed that, a 47.90% peak discharge increase (between 100 and 1000 year flood period, for 1-D steady flow analysis) results in a corresponding 14.78% increase in the floodplain area. This can be justified by the fact that the slopes of the basin areas along the river are steep enough to avert a "blow up" in the inundated areas.

As it concerns 2-D flow analysis, the difference in floodplain area between 50 and 100 year unsteady flow simulation is quite small (5.90%). It is not what expected, because 2-D analysis is more smooth than 1-D analysis.

Two-dimensional (2D) analysis, according to Table 12, results in a large floodplain area, in comparison to one-dimensional (1D) unsteady flow analysis. This can be explained by the fact that 1-D analysis presents larger depths than the 2-D analysis, as inundations maps indicate. This can be understood better by Figures 53 and 54, where depth for 1-D analysis is 4.00 and 6.00 meters above depth in 2-D analysis, for 50 and 100 years respectively. Where one-dimensional (1D) analysis results to large depths, two-dimensional (2D) analysis results in low depths, but to a more extended floodplain area.

The 2D mesh pre-processor computes a detailed elevation-volume relationship for each cell and each cell face of a computational cell is pre-processed into detailed hydraulic property tables. As shown in Figures 41 and 43, each cell is like a detailed cross-section. So the flow of water into, through, and out of a cell is controlled by the details of these properties and the cell level over other model, that use a single elevation for each cell and face, let alone a one-dimensional (1D) model, that is not so much detailed. Moreover, two-dimensional (2D) flow velocities can capture flow effects in a better way.

An assumption in the momentum equations, in 1-D analysis, is that the water surface is horizontal at any cross-section perpendicular to the flow. Therefore, the water surface elevation in one-dimensional (1D) flow analysis is the same for the channel and the floodplain at a given cross-section, and, possibly, is not capable of representing the overland.

At the upstream boundary (Figure 49), all simulations (1D and 2D), start and end up at the same depth (0.00 meters). At time-step 6:30, max depth is 1.79 meters for both one-dimensional and two-dimensional unsteady flow analysis, for 50 years flood period. At 6:15, max depth is, in approximation, 2.06 meters for both one-dimensional (1D) and

Institutional Repository - Library & Information Centre - University of Thessaly
20/05/2024 06:18:41 EEST - 3.23.102.234

two-dimensional (2D) flow analysis, for 100 years flood period. The difference in these two simulations (1-D and 2-D) is in the time that depth of water is zero again (time-step 17:23, for 2D, and time step 20:30, for 1-D, for 50 years flood period).

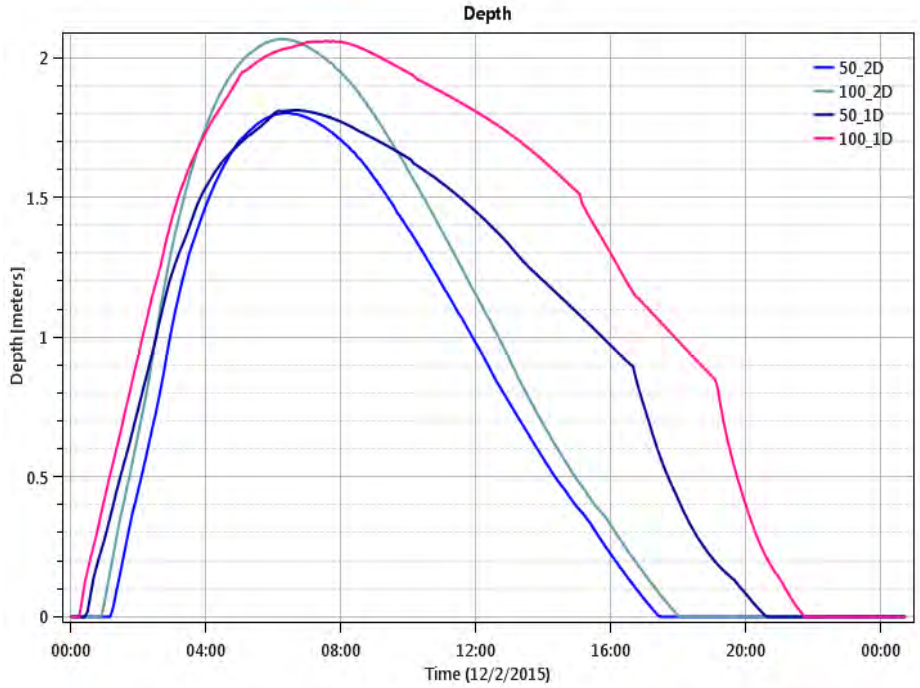

Figure 49. Time series hydrograph plot at the upstream of Titarisios River reach for the comparison one-dimensional (1D) and of two-dimensional (2D) simulation, for 50 and 100 years flood period.

Similarly, in two-dimensional (2D) flow analysis, water surface elevation (Figure 50) falls to zero about three hours earlier than in the one-dimensional (1D) flow analysis.

Institutional Repository - Library & Information Centre - University of Thessaly
20/05/2024 06:18:41 EEST - 3.23.102.234

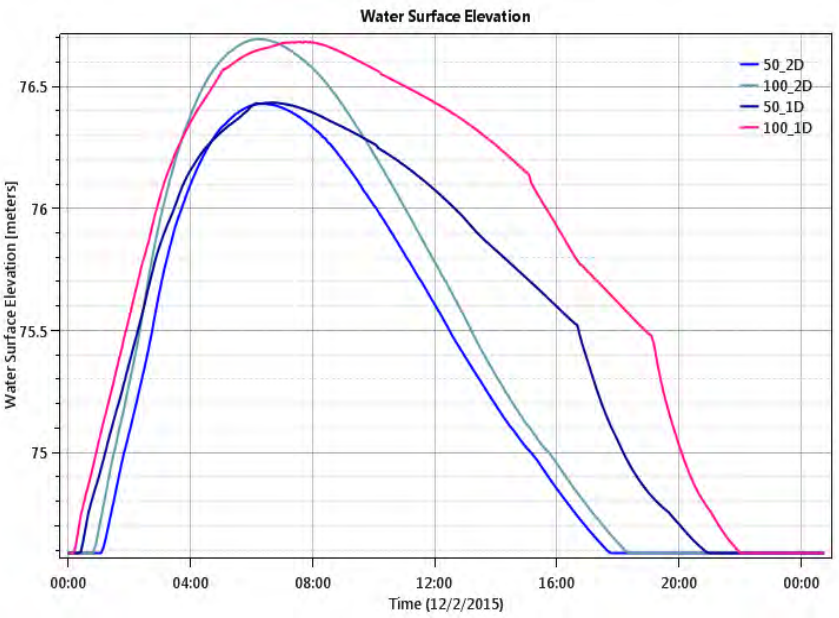

Figure 50. Time series hydrograph plot at the upstream of Titarisios River reach for the comparison one-dimensional (1D) and of two-dimensional (2D) simulation, for 50 and 100 years flood period.

On the other hand, at the downstream boundary (Figure 51), although 1-D and 2-D start at the same depth (3.35 meters, for 50 years flood period and 3.70 meters, for 100 years flood period). At time-step 12:45, max depth is 5.55 meters for one-dimensional (1D) and 5.95 meters for two-dimensional (2D) unsteady flow analysis, for 50 years flood period. Respectively, max depth is, in approximation, 5.60 meters for one-dimensional (1D) and 6.05 meters for two-dimensional (2D) unsteady flow analysis, for 100 years flood period. The difference in depth between one-dimensional and two-dimensional flow analysis remains until the end of the simulation, but with tend to convergence.

All the above can by concluded, also, by the water surface elevation versus time diagram (Figure 52).

Institutional Repository - Library & Information Centre - University of Thessaly
20/05/2024 06:18:41 EEST - 3.23.102.234

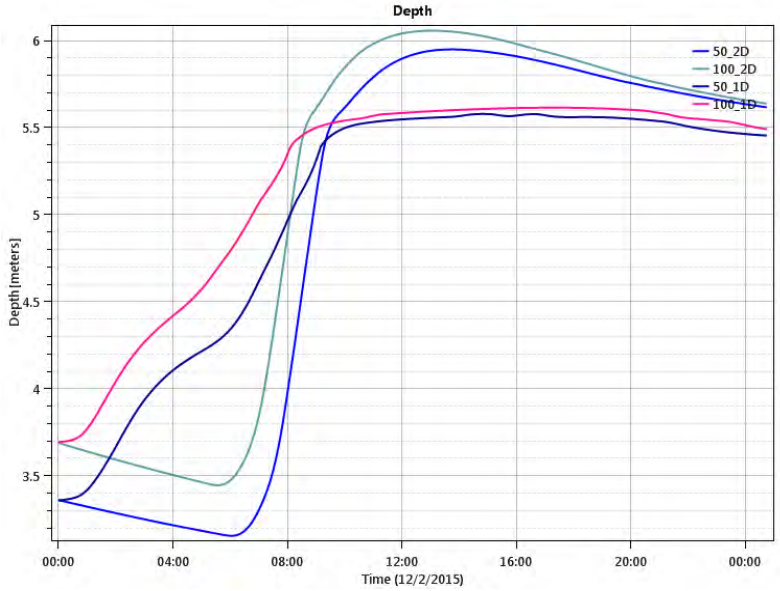

Figure 51. Time series hydrograph plot at the downstream of Titarisios River reach for the comparison one-dimensional (1D) and of two-dimensional (2D) simulation, for 50 and 100 years flood period.

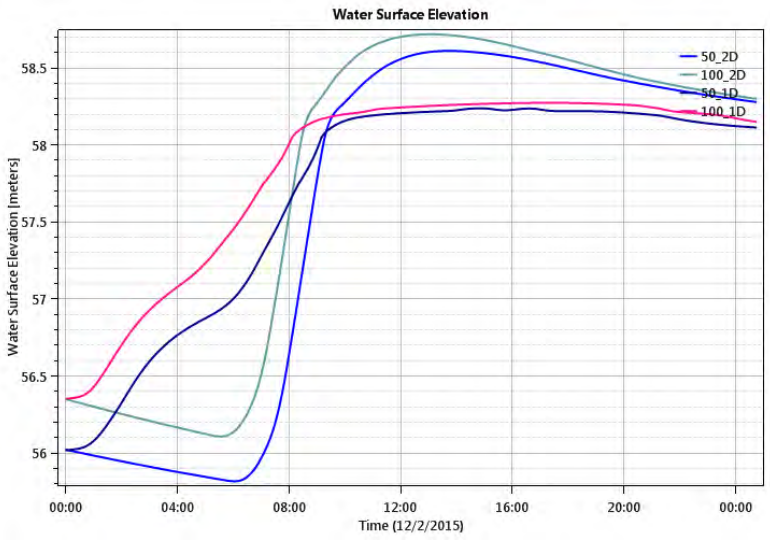

Figure 52. Time series hydrograph plot at the downstream of Titarisios River reach for the comparison one-dimensional (1D) and of two-dimensional (2D) simulation, for 50 and 100 years flood period.

Institutional Repository - Library & Information Centre - University of Thessaly
20/05/2024 06:18:41 EEST - 3.23.102.234

If we select a position among cross sections 7537.91 and 7301.85 (Figure 28), which have been flooded, we can state that depth (Figure 53), and water surface (Figure 54), estimated by one-dimensional (1D) flow analysis is greater than by two-dimensional (2D). One the opposite, two-dimensional (2D) flow analysis seems smoother than one-dimensional (1D) analysis.

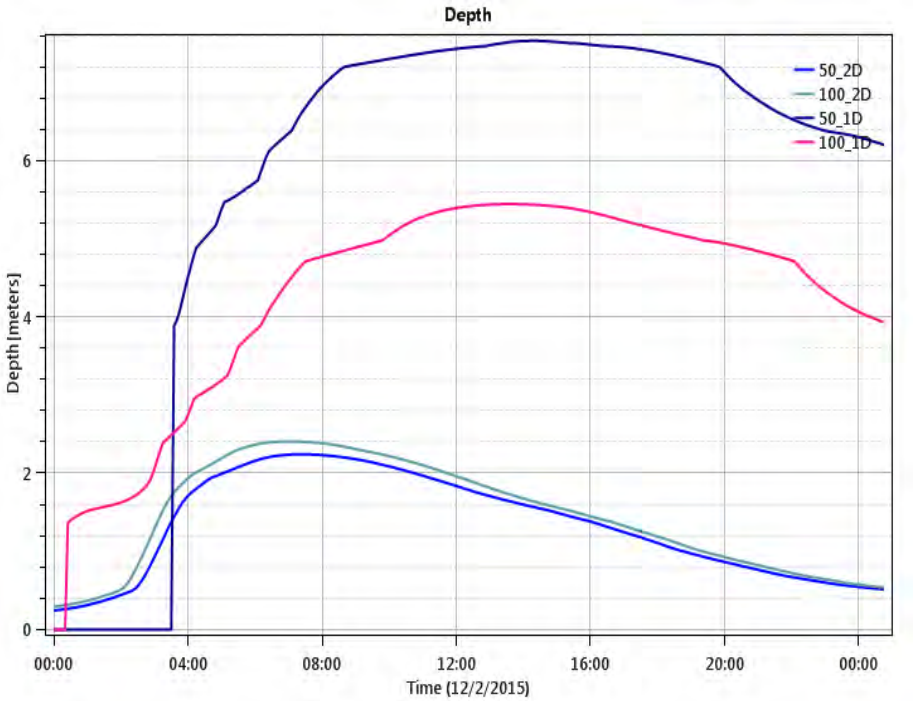

Figure 53. Time series hydrograph plot in the middle of Titarisios River reach for the comparison one-dimensional (1D) and of two-dimensional (2D) simulation, for 50 and 100 years flood period.

Institutional Repository - Library & Information Centre - University of Thessaly
20/05/2024 06:18:41 EEST - 3.23.102.234

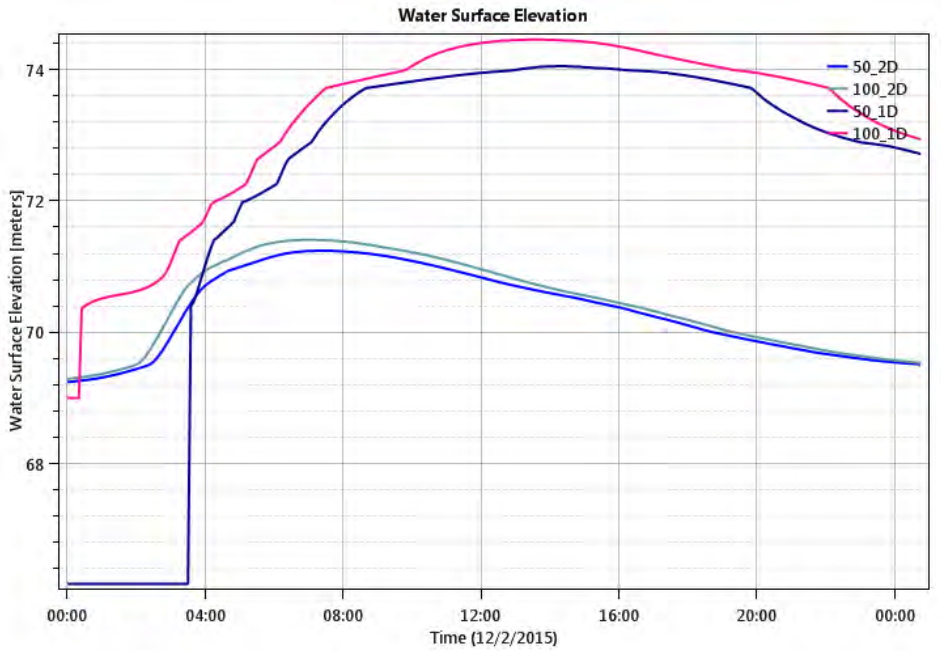

Figure 54. Time series hydrograph plot in the middle of Titarisios River reach for the comparison one-dimensional (1D) and of two-dimensional (2D) simulation, for 50 and 100 years flood period.

As mentioned above, in simulation at the upstream of Titarisios River Reach, depth and, thus, water surface elevation is similar for one-dimensional (1D) and two-dimensional (2D) flow analysis, for 50 and 100 years flood period. Because, boundary conditions are the same upstream and downstream the river, simulation at the downstream, is, also, quite, similar. The difference arise in the middle of Titarisios river, where the river is flooded, and we can conclude that two-dimensional (2D) simulation has smoother results than the one-dimensional (1D) analysis.

Institutional Repository - Library & Information Centre - University of Thessaly
20/05/2024 06:18:41 EEST - 3.23.102.234

4 CONCLUSIONS

The goal of our case-study is to design flood maps for flood risk assessment, for 50 and 100 years flood period, through hydrologic and hydraulic simulations, with the help of HEC-HMS and HEC-RAS programs, for Titarisios River Reach, in Thessaly. Moreover, a comparison of one-dimensional (1D) and two-dimensional (2D) unsteady flow analysis is necessary, in order to highlight the differences between these two simulations, for 50 and 100 years flood period, respectively. Some important conclusions about the methodology and the simulations are described as following:

The worst-design hydrograph (SCS transform method) was used to simulate hydraulic parameters of the river reach among the three synthetic unit hydrographs, SCS, Snyder and Clark.

Two terrains were created in order to derive basin characteristics and simulate Titarisios River Reach. Although the terrains were quite accurate, since they were based on ASTER GDEM v2 Worldwide Elevation Data, there was a small difficulty in topographic mapping of Titarisios River Reach, and a site plan is necessary, so as to achieve perfect results. Nevertheless, the results of the simulations are quite sufficient.

One-dimensional (1D) and two-dimensional (2D) unsteady flow simulations were performed with exactly the same initial and boundary conditions, in order to be comparable.

Inundation maps were designed, by 1-D and 2-D simulations, for 50 and 100 years flood period. It is obvious from the results of the maps, that with the simulation for 100 years flood period flood area is increased at about 25,43%, in comparison with the simulation for 50 years flood period, as it regards one-dimensional (1D) unsteady flow analysis. On the other hand, the difference between 50 years and 100 years flood period is about 5.90%, for two-dimensional unsteady flow analysis (2D).

2-D simulation used a 2D flow area, where Saint Venant equation computes flow, velocities, and water surface elevation along x and y direction. This is important, because, two-dimensional (2D) model is capable of representing the flood area, while, 1-D model can be realistic in flow variables along the channel, but that, when it comes to the projection onto a 2D map, the representation of the terrain topography together with the mapping techniques that are employed introduce a limiting factor in their successful application, as Vojinovica et al (2009) state, also.

5 FUTURE WORK

As floods occur more and more often, causing a lot of damages in properties, and human's lives are at risk, flood risk management should focus on prevention, protection and preparedness. Flood risk assessments should include all the rivers of the member states, according to Directive 2007/60/EC. Moreover, the requirement of an accurate inundation mapping is essential to have a detailed topographic map, for the river reaches. These two goals could be achieved in the future studies.

Institutional Repository - Library & Information Centre - University of Thessaly
20/05/2024 06:18:41 EEST - 3.23.102.234

REFERENCES

Brunner Gury W., Hydrologic Engineering Center, Combined 1D and 2D modeling with HECRAS, USA, October 2014.

Cook A., Merwade V., Effect of topographic data, geometric configuration and modeling approach on flood inundation mapping, Journal of Hydrology Volume 377, Issues 1–2, , 20 October 2009.

Delaney P., Qiao Y., Using detailed 2D urban floodplain modeling to inform development planning in Mississauga, ON, 22nd Canadian Hydrotechnical Conference, *Water for sustainable development: Coping with Climate and environmental Changes*, Montreal, Quebec, April 29-May 2, 2015.

Directive 2007/60/EC of the European Parliament and of the Council of 23 October 2007 on the assessment and management of flood risks, Strasbourg, October 2007.

Giokas A.E., Training methodological framework to produce maps flood; *Applied on Regional Unit of Arcadia*, Athens, 2009.

Leandro, J., Chen, A., Djordjevij, S., and Savij, D., Comparison of 1D/1D and 1D/2D Coupled (Sewer/Surface) Hydraulic Models for Urban Flood Simulation, J. Hydraul. Eng., 10.1061/(ASCE)HY.1943-7900.0000037, 495-504, 2009.

Paraskevas I., Moukos A., Farsirotou E., Loukas A., Hydrologic and hydraulic simulation and composing flood maps, *Integrated water resources management in new era*, 3rd Conference, Athens, December 10-12, 2015.

US Army Corps of Engineers, Institute for water resources, Hydrologic Engineering Center, *HEC-RAS River Analysis System*, User's Manual, Version 4.1, 2010.

US Army Corps of Engineers, Institute for water resources Hydrologic Engineering Center, *HEC-RAS River Analysis System*, Hydraulic Reference Manual, Version 4.1, 2010.

US Army Corps of Engineers, Institute for water resources Hydrologic Engineering Center, *HEC-RAS River Analysis System*, Applications Guide, Version 4.1, 2010.

US Army Corps of Engineers, Institute for water resources Hydrologic Engineering Center, *HEC-RAS River Analysis System*, 2-D modeling User's Manual, Version 5.0 Beta, August 2015.

Venkatesh Merwade, Tutorial on using HEC-GeoRAS with ArcGIS 10 and HEC-RAS Modeling, *School of Civil Engineering*, Purdue University Georgia, 2012.

Verwey A., Latest Developments in Floodplain Modeling - 1D/2D Integration [online]. In: Conference on Hydraulics in Civil Engineering (6th: 2001: Hobart, Tas.). 6th Conference on Hydraulics in Civil Engineering: *The State of Hydraulics; Proceedings*. Barton, A.C.T.: Institution of Engineers, Australia, 2001: 13-24.

Vojinovica Z., Tutulica D., On the use of 1D and coupled 1D-2D modeling approaches for assessment of flood damage in urban areas, Urban Water Journal, Volume 6, Issue 3, 2009.

Ward R.C., Principles of Hydrology, McGraw-Hill Book Company Limited, United Kingdom, London, 1975.

Institutional Repository - Library & Information Centre - University of Thessaly
20/05/2024 06:18:41 EEST - 3.23.102.234

APPENDIX

Table A1. The alternating block model (Chow et al., 1988), for 50 yrs flood period.

k	t_r* (h)	t_r* (min)	h_1	φ	h1*φ	Δh	Rearrangement	P (mm)
1	0.25	15	22.902	0.498	11.396	11.396	0.378	0.378
2	0.5	30	32.452	0.606	19.660	8.264	0.390	0.768
3	0.75	45	38.360	0.658	25.240	5.580	0.402	1.170
4	1	60	42.627	0.691	29.444	4.204	0.415	1.585
5	1.25	75	45.971	0.714	32.822	3.378	0.429	2.014
6	1.5	90	48.729	0.732	35.653	2.830	0.445	2.458
7	1.75	105	51.081	0.746	38.093	2.441	0.461	2.920
8	2	120	53.136	0.757	40.243	2.149	0.479	3.399
9	2.25	135	54.964	0.767	42.166	1.923	0.499	3.898
10	2.5	150	56.614	0.776	43.909	1.743	0.521	4.419
11	2.75	165	58.119	0.783	45.504	1.595	0.545	4.963
12	3	180	59.505	0.789	46.976	1.472	0.571	5.534
13	3.25	195	60.790	0.795	48.345	1.368	0.600	6.134
14	3.5	210	61.989	0.801	49.624	1.279	0.634	6.768
15	3.75	225	63.115	0.805	50.825	1.201	0.671	7.439
16	4	240	64.176	0.810	51.958	1.134	0.714	8.153
17	4.25	255	65.180	0.814	53.032	1.073	0.763	8.917
18	4.5	270	66.134	0.817	54.052	1.020	0.821	9.738
19	4.75	285	67.042	0.821	55.024	0.972	0.890	10.628
20	5	300	67.910	0.824	55.953	0.929	0.972	11.600
21	5.25	315	68.741	0.827	56.843	0.890	1.073	12.673
22	5.5	330	69.539	0.830	57.697	0.854	1.201	13.875
23	5.75	345	70.306	0.832	58.518	0.821	1.368	15.243
24	6	360	71.045	0.835	59.309	0.791	1.595	16.838
25	6.25	375	71.758	0.837	60.073	0.763	1.923	18.762
26	6.5	390	72.447	0.839	60.810	0.738	2.441	21.202
27	6.75	405	73.114	0.841	61.524	0.714	3.378	24.581
28	7	420	73.761	0.843	62.216	0.692	5.580	30.161
29	7.25	435	74.388	0.845	62.887	0.671	11.396	41.557
30	7.5	450	74.997	0.847	63.539	0.652	8.264	49.821
31	7.75	465	75.589	0.849	64.173	0.634	4.204	54.025
32	8	480	76.166	0.851	64.789	0.617	2.830	56.855
33	8.25	495	76.728	0.852	65.390	0.600	2.149	59.004
34	8.5	510	77.275	0.854	65.975	0.585	1.743	60.747
35	8.75	525	77.809	0.855	66.546	0.571	1.472	62.219
36	9	540	78.331	0.857	67.104	0.557	1.279	63.498

Institutional Repository - Library & Information Centre - University of Thessaly
20/05/2024 06:18:41 EEST - 3.23.102.234

k	t_r* (h)	t_r* (min)	h_1	φ	h1*φ	Δh	Rearrangement	P (mm)
37	9.25	555	78.841	0.858	67.648	0.545	1.134	64.632
38	9.5	570	79.339	0.859	68.180	0.532	1.020	65.652
39	9.75	585	79.827	0.861	68.701	0.521	0.929	66.581
40	10	600	80.304	0.862	69.211	0.510	0.854	67.435
41	10.25	615	80.772	0.863	69.710	0.499	0.791	68.226
42	10.5	630	81.230	0.864	70.199	0.489	0.738	68.964
43	10.75	645	81.679	0.865	70.678	0.479	0.692	69.656
44	11	660	82.120	0.866	71.148	0.470	0.652	70.307
45	11.25	675	82.552	0.867	71.609	0.461	0.617	70.924
46	11.5	690	82.977	0.868	72.062	0.453	0.585	71.509
47	11.75	705	83.394	0.869	72.506	0.445	0.557	72.067
48	12	720	83.804	0.870	72.943	0.437	0.532	72.599
49	12.25	735	84.207	0.871	73.372	0.429	0.510	73.109
50	12.5	750	84.604	0.872	73.794	0.422	0.489	73.597
51	12.75	765	84.993	0.873	74.209	0.415	0.470	74.067
52	13	780	85.377	0.874	74.618	0.408	0.453	74.520
53	13.25	795	85.755	0.875	75.020	0.402	0.437	74.957
54	13.5	810	86.127	0.876	75.415	0.396	0.422	75.379
55	13.75	825	86.493	0.876	75.805	0.390	0.408	75.787
56	14	840	86.854	0.877	76.189	0.384	0.396	76.183
57	14.25	855	87.209	0.878	76.567	0.378	0.384	76.567
58	14.5	870	87.560	0.879	76.939	0.373	0.373	76.939

Institutional Repository - Library & Information Centre - University of Thessaly
20/05/2024 06:18:41 EEST - 3.23.102.234

Table A2. Alternating block model (Chow et al., 1988), for 100 yrs flood period

k	t_r* (h)	t_r* (min)	h_1	φ	h1*φ	Δh	Rearrangement	P (mm)
1	0.25	15	25.0497	0.498	12.465	12.465	0.414	0.414
2	0.5	30	35.4946	0.606	21.504	9.039	0.426	0.840
3	0.75	45	41.9571	0.658	27.607	6.103	0.440	1.279
4	1	60	46.6238	0.691	32.205	4.598	0.454	1.733
5	1.25	75	50.2819	0.714	35.900	3.695	0.469	2.203
6	1.5	90	53.2979	0.732	38.996	3.096	0.486	2.689
7	1.75	105	55.8702	0.746	41.665	2.669	0.504	3.193
8	2	120	58.1178	0.757	44.016	2.351	0.524	3.718
9	2.25	135	60.1176	0.767	46.120	2.104	0.546	4.263
10	2.5	150	61.922	0.776	48.026	1.906	0.569	4.833
11	2.75	165	63.5683	0.783	49.771	1.745	0.596	5.428
12	3	180	65.0839	0.789	51.381	1.610	0.625	6.053
13	3.25	195	66.4896	0.795	52.878	1.496	0.657	6.710
14	3.5	210	67.8016	0.801	54.276	1.399	0.693	7.403
15	3.75	225	69.0326	0.805	55.590	1.314	0.734	8.137
16	4	240	70.1931	0.810	56.830	1.240	0.781	8.918
17	4.25	255	71.2914	0.814	58.004	1.174	0.835	9.753
18	4.5	270	72.3344	0.817	59.120	1.116	0.898	10.651
19	4.75	285	73.3281	0.821	60.183	1.063	0.973	11.624
20	5	300	74.2773	0.824	61.199	1.016	1.063	12.688
21	5.25	315	75.1864	0.827	62.172	0.973	1.174	13.862
22	5.5	330	76.0588	0.830	63.106	0.934	1.314	15.176
23	5.75	345	76.8977	0.832	64.005	0.898	1.496	16.672
24	6	360	77.706	0.835	64.870	0.865	1.745	18.417
25	6.25	375	78.486	0.837	65.705	0.835	2.104	20.521
26	6.5	390	79.2399	0.839	66.512	0.807	2.669	23.190
27	6.75	405	79.9695	0.841	67.293	0.781	3.695	26.885
28	7	420	80.6766	0.843	68.050	0.757	6.103	32.989
29	7.25	435	81.3627	0.845	68.784	0.734	12.465	45.453
30	7.5	450	82.029	0.847	69.497	0.713	9.039	54.492
31	7.75	465	82.6769	0.849	70.190	0.693	4.598	59.090
32	8	480	83.3075	0.851	70.864	0.674	3.096	62.186
33	8.25	495	83.9218	0.852	71.521	0.657	2.351	64.537
34	8.5	510	84.5207	0.854	72.161	0.640	1.906	66.443
35	8.75	525	85.105	0.855	72.786	0.625	1.610	68.053
36	9	540	85.6756	0.857	73.396	0.610	1.399	69.452
37	9.25	555	86.2331	0.858	73.991	0.596	1.240	70.692

Institutional Repository - Library & Information Centre - University of Thessaly
20/05/2024 06:18:41 EEST - 3.23.102.234

k	t_r* (h)	t_r* (min)	h_1	φ	h1*φ	Δh	Rearrangement	P (mm)
38	9.5	570	86.7782	0.859	74.573	0.582	1.116	71.808
39	9.75	585	87.3115	0.861	75.143	0.569	1.016	72.824
40	10	600	87.8336	0.862	75.700	0.557	0.934	73.758
41	10.25	615	88.345	0.863	76.246	0.546	0.865	74.623
42	10.5	630	88.8462	0.864	76.781	0.535	0.807	75.430
43	10.75	645	89.3376	0.865	77.305	0.524	0.757	76.187
44	11	660	89.8197	0.866	77.819	0.514	0.713	76.900
45	11.25	675	90.2928	0.867	78.323	0.504	0.674	77.574
46	11.5	690	90.7574	0.868	78.818	0.495	0.640	78.214
47	11.75	705	91.2137	0.869	79.305	0.486	0.610	78.824
48	12	720	91.662	0.870	79.782	0.478	0.582	79.406
49	12.25	735	92.1028	0.871	80.252	0.469	0.557	79.963
50	12.5	750	92.5363	0.872	80.713	0.462	0.535	80.498
51	12.75	765	92.9627	0.873	81.167	0.454	0.514	81.012
52	13	780	93.3823	0.874	81.614	0.447	0.495	81.507
53	13.25	795	93.7954	0.875	82.054	0.440	0.478	81.985
54	13.5	810	94.2021	0.876	82.486	0.433	0.462	82.447
55	13.75	825	94.6028	0.876	82.912	0.426	0.447	82.893
56	14	840	94.9975	0.877	83.332	0.420	0.433	83.326
57	14.25	855	95.3865	0.878	83.746	0.414	0.420	83.746
58	14.5	870	95.77	0.879	84.153	0.408	0.408	84.153

Institutional Repository - Library & Information Centre - University of Thessaly
20/05/2024 06:18:41 EEST - 3.23.102.234

Table A3. CN for Land Cover Corine 2000 (Fausto Miliani,Giovanni Ravazzani, Marco Mancini)

CORINE land cover class	Hydrologic soil group			
	A	B	C	D
Continuous urban fabric	89	92	94	95
Discontinuous urban fabric	77	85	90	92
Industrial or commercial units	81	88	91	93
Road and rail networks and associated land	98	98	98	98
Port areas	81	88	91	93
Airports	72	82	87	89
Mineral extraction sites	72	82	87	89
Dump sites	72	82	87	89
Construction sites	72	82	87	89
Green urban areas	68	79	86	89
Sport and leisure facilities	49	69	79	84
Nonirrigated arable land	49	69	79	84
Permanently irrigated land	49	69	79	84
Rice fields	59	70	78	81
Vineyards	67	77	83	87
Fruit trees and berry plantations	65	75	82	86
Olive groves	65	75	82	86
Pastures	49	69	79	84
Annual crops associatedwith permanent crops	62	71	78	81
Complex cultivation patterns	67	78	85	89
Land principally occupied by agriculture, with significant areas of natural vegetation	67	78	85	89

Institutional Repository - Library & Information Centre - University of Thessaly
20/05/2024 06:18:41 EEST - 3.23.102.234

CORINE land cover class	Hydrologic soil group			
Agroforestry areas	45	66	77	83
Broad-leaved forest	60	65	70	77
Coniferous forest	60	65	70	77
Mixed forest	60	65	70	77
Natural grassland	60	65	74	80
Moors and heathland	60	65	74	80
Sclerophyllous vegetation	60	65	74	80
Transitional woodland-scrub	60	65	74	80
Beaches, dunes, sands	25	55	70	77
Bare rocks	68	79	86	89
Sparsely vegetated areas	68	79	86	89
Burnt areas	68	79	86	89
Glaciers and perpetual snow	79	79	79	79
Inland marshes	98	98	98	98
Water courses	99	99	99	99
Water bodies	99	99	99	99
Coastal lagoons	99	99	99	99

Institutional Repository - Library & Information Centre - University of Thessaly
20/05/2024 06:18:41 EEST - 3.23.102.234

Table A4. Manning's n values according to Corine Land Cover 2000

Corine Land Cover	n Value
Continuous urban fabric	0.1
Discontinuous urban fabric	0.1
Industrial or commercial units	0.1
Road and rail networks and associated land	0.1
Airports	0.1
Mineral extraction sites	0.1
Nonirrigated arable land	0.03
Permanently irrigated land	0.035
Rice fields	0.035
Vineyards	0.04
Fruit trees and berry plantations	0.05
Olive groves	0.05
Pastures	0.05
Complex cultivation patterns	0.055
Land principally occupied by agriculture, with significant areas of natural vegetation	0.055
Broad-leaved forest	0.055
Coniferous forest	0.055
Natural grassland	0.035
Sclerophyllous vegetation	0.05
Transitional woodland-scrub	0.05
Beaches, dunes, sands	0.04
Sparsely vegetated areas	0.04
Inland marshes	0.04
Water courses	0.04

Institutional Repository - Library & Information Centre - University of Thessaly
20/05/2024 06:18:41 EEST - 3.23.102.234

Table A5. Results of one-dimensional (1D) unsteady flow analysis, for 50 and 100 yrs flood period

Reach	River Station	Profile	Plan	Q Total	Min Ch El	W.S. Elev	Crit W.S.	E.G. Elev	E.G. Slope	Vel Chnl	Flow Area	Top Width	Froude
				(m3/s)	(m)	(m)	(m)	(m)	(m/m)	(m/s)	(m2)	(m)	
Titarisios	8825.314	max ws	100_1D	887.02	73.72	76.69		77.24	0.0063	3.29	275.47	147.91	0.72
Titarisios	8825.314	max ws	50_1D	769.54	73.72	76.44		76.98	0.007232	3.25	239.72	140.51	0.75
Titarisios	8708.497	max ws	100_1D	606.18	73.2	76.4		76.49	0.000971	1.4	443.5	206.86	0.29
Titarisios	8708.497	max ws	50_1D	511.91	73.2	75.99		76.09	0.001308	1.43	361.57	194.57	0.32
Titarisios	8531.981	max ws	100_1D	540.72	72.8	76.34		76.34	0.000001	0.05	12127.2	2566.49	0.01
Titarisios	8531.981	max ws	50_1D	484.67	72.8	75.93		75.94	0.000056	0.38	1273.45	456.4	0.07
Titarisios	8380.813	max ws	100_1D	540.15	72.4	76.34		76.34	0.000001	0.04	13144.9	2424.03	0.01
Titarisios	8380.813	max ws	50_1D	484.04	72.4	75.93		75.93	0.000001	0.04	12165.8	2410.7	0.01
Titarisios	8242.008	max ws	100_1D	540.3	72	76.34		76.34	0	0.03	17955	3968.38	0.01
Titarisios	8242.008	max ws	50_1D	483.53	72	75.93		75.93	0	0.04	13105.2	2432.33	0.01
Titarisios	8119.165	max ws	100_1D	540.16	71.6	76.34		76.34	0.000004	0.13	5778.75	1521.53	0.02
Titarisios	8119.165	max ws	50_1D	483.68	71.6	75.93		75.93	0.000004	0.13	5171.97	1427.54	0.02
Titarisios	8028.381	max ws	100_1D	539.87	71.21	76.33		76.56	0.001042	2.09	258.54	59.31	0.32
Titarisios	8028.381	max ws	50_1D	483.58	71.21	75.93		76.15	0.001116	2.06	234.76	58.06	0.33
Titarisios	7929.131	max ws	100_1D	516.87	70.8	75.56	76.03	77.31	0.014265	5.87	88.08	29.17	1.08
Titarisios	7929.131	max ws	50_1D	474.84	70.8	75.09	75.45	77.08	0.015583	6.25	75.98	24.18	1.13
Titarisios	7818.051	max ws	100_1D	500.31	70.4	74.74		74.76	0.000097	0.58	946.49	338.93	0.1
Titarisios	7818.051	max ws	50_1D	412.93	70.4	74.29		74.31	0.000108	0.56	798.52	320.29	0.1
Titarisios	7537.909	max ws	100_1D	499.97	70	74.74		74.74	0	0.03	17131.7	3842.78	0.01
Titarisios	7537.909	max ws	50_1D	412.75	70	74.29		74.29	0	0.03	15421.4	3747.97	0
Titarisios	7301.85	max ws	100_1D	499.98	69.6	74.74		74.74	0	0.04	16928	4055.19	0.01

Institutional Repository - Library & Information Centre - University of Thessaly
20/05/2024 06:18:41 EEST - 3.23.102.234

Reach	River Station	Profile	Plan	Q Total	Min Ch El	W.S. Elev	Crit W.S.	E.G. Elev	E.G. Slope	Vel Chnl	Flow Area	Top Width	Froude
Titarisios	7301.85	max ws	50_1D	412.82	69.6	74.29		74.29	0	0.03	15121.5	3969.31	0.01
Titarisios	7190.67	max ws	100_1D	499.96	69.2	74.74		74.74	0	0.03	10222.9	2276.89	0.01
Titarisios	7190.67	max ws	50_1D	412.8	69.2	74.29		74.29	0	0.03	9222.25	2186.65	0.01
Titarisios	7081.276	max ws	100_1D	499.94	68.8	74.15	73.92	75.66	0.010887	5.45	91.72	27.29	0.95
Titarisios	7081.276	max ws	50_1D	412.55	68.8	73.8		75.06	0.009007	4.98	82.8	24.24	0.86
Titarisios	6945.251	max ws	100_1D	499.93	68.4	73.34		73.52	0.001026	1.85	270.39	74.62	0.31
Titarisios	6945.251	max ws	50_1D	412.51	68.4	73.13		73.26	0.000757	1.62	255.23	68.49	0.27
Titarisios	6730.716	max ws	100_1D	499.93	68	72.09		72.98	0.01067	4.16	120.13	57.56	0.92
Titarisios	6730.716	max ws	50_1D	412.28	68	71.76	71.67	72.6	0.011607	4.06	101.48	53.67	0.94
Titarisios	6588.549	max ws	100_1D	499.91	67.6	71.21		71.66	0.003101	2.96	168.63	51.73	0.52
Titarisios	6588.549	max ws	50_1D	411.94	67.6	70.83		71.22	0.003083	2.76	149.02	50.79	0.52
Titarisios	6451.33	max ws	100_1D	499.88	67.2	70.65		71.48	0.006778	4.03	124.17	43.27	0.76
Titarisios	6451.33	max ws	50_1D	403.42	67.2	70.39		71.04	0.005849	3.58	112.82	42.17	0.7
Titarisios	6309.623	max ws	100_1D	499.82	66.81	70.17	70.27	71.8	0.01343	5.66	88.23	29.6	1.05
Titarisios	6309.623	max ws	50_1D	400.63	66.81	70.05		71.19	0.009774	4.73	84.63	29.36	0.89
Titarisios	6189.648	max ws	100_1D	425.57	66.44	69.7	70.98	73.83	0.161096	9	47.3	25.43	2.11
Titarisios	6189.648	max ws	50_1D	408.67	66.44	69.67	70.91	73.58	0.153632	8.76	46.67	25.32	2.06
Titarisios	6024.187	max ws	100_1D	404.36	66	69.33		69.78	0.003601	2.97	136.02	45.78	0.55
Titarisios	6024.187	max ws	50_1D	392.93	66	69.32		69.75	0.003409	2.89	135.91	45.77	0.54
Titarisios	5914.62	max ws	100_1D	409.95	65.4	69.32		69.63	0.001962	2.46	166.62	47.75	0.42
Titarisios	5914.62	max ws	50_1D	406.13	65.4	69.32		69.62	0.001929	2.44	166.51	47.74	0.42
Titarisios	5797.133	max ws	100_1D	484.97	65.01	69.06		69.5	0.007862	2.93	165.35	107.72	0.75
Titarisios	5797.133	max ws	50_1D	593.65	65.01	68.98	68.97	69.71	0.013891	3.8	156.22	105.16	1

Institutional Repository - Library & Information Centre - University of Thessaly
20/05/2024 06:18:41 EEST - 3.23.102.234

Reach	River Station	Profile	Plan	Q Total	Min Ch El	W.S. Elev	Crit W.S.	E.G. Elev	E.G. Slope	Vel Chnl	Flow Area	Top Width	Froude
Titarisios	5691.386	max ws	100_1D	543.78	64.6	69.04		69.51	0.002678	3.04	178.73	46.89	0.5
Titarisios	5691.386	max ws	50_1D	542.91	64.6	69.03		69.51	0.002673	3.04	178.65	46.89	0.5
Titarisios	5572.422	max ws	100_1D	542.65	64.21	68.5		69.52	0.006261	4.46	121.86	35.05	0.76
Titarisios	5572.422	max ws	50_1D	540.88	64.21	68.5		69.51	0.006239	4.45	121.75	35.05	0.76
Titarisios	5462.955	max ws	100_1D	535.81	63.8	68.15		68.55	0.002223	2.82	190.02	44.73	0.44
Titarisios	5462.955	max ws	50_1D	533.62	63.8	68.15		68.55	0.002198	2.81	190.21	44.73	0.43
Titarisios	5328.467	max ws	100_1D	484.9	63.4	67.41	67.37	68.82	0.011562	5.25	92.4	31.61	0.98
Titarisios	5328.467	max ws	50_1D	530.86	63.4	67.39	67.58	69.1	0.014208	5.8	91.56	31.49	1.09
Titarisios	5165.88	max ws	100_1D	484.89	62.86	67.43		67.56	0.001129	1.61	301.51	113.44	0.32
Titarisios	5165.88	max ws	50_1D	464.69	62.86	67.35		67.48	0.00113	1.59	292.4	112.02	0.31
Titarisios	5008.994	max ws	100_1D	484.88	62.6	67.26		67.38	0.001214	1.49	325.6	145.27	0.32
Titarisios	5008.994	max ws	50_1D	464.77	62.6	67.18		67.29	0.001234	1.48	313.5	142.52	0.32
Titarisios	4835.389	max ws	100_1D	484.87	62.2	67.02		67.13	0.001631	1.51	320.24	173.88	0.36
Titarisios	4835.389	max ws	50_1D	459.52	62.2	66.94		67.05	0.001606	1.5	306.87	167.48	0.35
Titarisios	4665.267	max ws	100_1D	484.86	61.8	66.94		66.97	0.000144	0.68	739.74	290.32	0.12
Titarisios	4665.267	max ws	50_1D	457.18	61.8	66.87		66.89	0.000139	0.65	717.91	284.79	0.11
Titarisios	4418.614	max ws	100_1D	484.86	61.4	66.94		66.94	0.00002	0.28	1705.74	421.68	0.05
Titarisios	4418.614	max ws	50_1D	452.16	61.4	66.86		66.87	0.000018	0.27	1674.19	419.73	0.04
Titarisios	4176.894	max ws	100_1D	484.85	61.01	66.25		66.52	0.005168	2.31	209.63	142.31	0.61
Titarisios	4176.894	max ws	50_1D	447.72	61.01	66.11		66.39	0.005718	2.35	190.8	136.7	0.63
Titarisios	4031.152	max ws	100_1D	484.85	60.6	65.88		65.99	0.001395	1.44	336.76	174.43	0.33
Titarisios	4031.152	max ws	50_1D	446.96	60.6	65.68		65.79	0.001611	1.48	302.39	166.28	0.35

Institutional Repository - Library & Information Centre - University of Thessaly
20/05/2024 06:18:41 EEST - 3.23.102.234

Reach	River Station	Profile	Plan	Q Total	Min Ch El	W.S. Elev	Crit W.S.	E.G. Elev	E.G. Slope	Vel Chnl	Flow Area	Top Width	Froude
Titarisios	3895.073	max ws	100_1D	484.84	60.2	65.85		65.87	0.000117	0.63	778.48	241.57	0.11
Titarisios	3895.073	max ws	50_1D	441.9	60.2	65.64		65.66	0.00012	0.62	727.95	238.21	0.11
Titarisios	3724.836	max ws	100_1D	484.84	59.8	63.74	64.41	65.67	0.024639	6.15	78.88	37.57	1.35
Titarisios	3724.836	max ws	50_1D	441.24	59.8	63.58	64.19	65.44	0.024225	6.04	73.01	35.11	1.34
Titarisios	3482.831	max ws	100_1D	484.75	59.4	60.68		60.71	0.000741	0.77	625.8	515.44	0.22
Titarisios	3482.831	max ws	50_1D	439.8	59.4	60.58		60.61	0.00081	0.77	573.63	512.65	0.23
Titarisios	3271.008	max ws	100_1D	484.72	59	60.6		60.61	0.000211	0.48	1030.02	728.64	0.12
Titarisios	3271.008	max ws	50_1D	436.25	59	60.49		60.5	0.000221	0.47	950.76	723.77	0.13
Titarisios	2898.824	max ws	100_1D	484.68	58.6	60.29		60.36	0.001195	1.18	412.3	259.66	0.3
Titarisios	2898.824	max ws	50_1D	435.34	58.6	60.18		60.25	0.001218	1.14	383.2	257.76	0.3
Titarisios	2725.757	max ws	100_1D	484.35	58	59.73		59.97	0.003962	2.14	226.24	142.3	0.54
Titarisios	2725.757	max ws	50_1D	435.27	58	59.62		59.84	0.004008	2.06	210.82	141.24	0.54
Titarisios	2524.466	max ws	100_1D	482.99	57	59.36		59.39	0.000379	0.84	651.85	378.85	0.18
Titarisios	2524.466	max ws	50_1D	430.93	57	59.24		59.27	0.000372	0.8	607.97	372.84	0.17
Titarisios	2281.883	max ws	100_1D	482.58	56	59.33		59.33	0.000038	0.32	1978.13	1221.43	0.06
Titarisios	2281.883	max ws	50_1D	422.86	56	59.21		59.21	0.000037	0.3	1836.42	1219.08	0.06
Titarisios	2097.272	max ws	100_1D	482.65	55.5	59.32		59.33	0.000087	0.5	1181.13	618.89	0.09
Titarisios	2097.272	max ws	50_1D	422.01	55.5	59.2		59.21	0.00008	0.47	1104.17	615.81	0.09
Titarisios	1930.351	max ws	100_1D	482.62	55	59.31		59.32	0.000106	0.62	1033.37	685.13	0.1
Titarisios	1930.351	max ws	50_1D	422.07	55	59.18		59.19	0.000095	0.58	948.87	678.24	0.1
Titarisios	1682.989	max ws	100_1D	482.62	55.03	58.99		59.12	0.001751	1.76	333.35	243.41	0.38
Titarisios	1682.989	max ws	50_1D	421.99	55.03	58.89		59.01	0.001658	1.66	308.87	240.29	0.37
Titarisios	1387.944	max ws	100_1D	482.61	54.5	58.67		58.75	0.000713	1.24	389.7	153.65	0.25

Institutional Repository - Library & Information Centre - University of Thessaly
20/05/2024 06:18:41 EEST - 3.23.102.234

Reach	River Station	Profile	Plan	Q Total	Min Ch El	W.S. Elev	Crit W.S.	E.G. Elev	E.G. Slope	Vel Chnl	Flow Area	Top Width	Froude
Titarisios	1387.944	max ws	50_1D	421.96	54.5	58.61		58.67	0.000585	1.11	379.84	151.64	0.22
Titarisios	1176.646	max ws	100_1D	482.6	54	58.58		58.62	0.000489	0.94	513.18	231.2	0.2
Titarisios	1176.646	max ws	50_1D	421.85	54	58.53		58.57	0.000399	0.84	502.22	230.14	0.18
Titarisios	873.348	max ws	100_1D	482.6	53	58.52		58.53	0.000086	0.58	877.9	322.73	0.09
Titarisios	873.348	max ws	50_1D	421.72	53	58.48		58.49	0.000068	0.51	866.28	318.39	0.08
Titarisios	661.8054	max ws	100_1D	482.6	52.68	58.52		58.52	0.000021	0.31	1572.17	377.66	0.05
Titarisios	661.8054	max ws	50_1D	421.69	52.68	58.48		58.48	0.000017	0.27	1558.51	375.62	0.04
Titarisios	319.4476	max ws	100_1D	482.59	52.4	58.27	57.1	58.29	0.001641	0.44	938.93	2473.52	0.19
Titarisios	319.4476	max ws	50_1D	421.61	52.4	58.24	56.94	58.25	0.001769	0.43	850.02	2470.59	0.19

Institutional Repository - Library & Information Centre - University of Thessaly
20/05/2024 06:18:41 EEST - 3.23.102.234